A DUMMY HEAD AND NECK MODEL FOR BOTH FRONTAL AND REAR IMPACTS

ÖNDEN VE ARKADAN ÇARPIŞMALAR İÇİN BİR MANKEN KAFA-BOYUN MODELİ

YASİN DEMİRER

ASSIST. PROF. DR. SELÇUK HİMMETOĞLU

Supervisor

Submitted to Graduate School of Science and Engineering of Hacettepe University

as a Partial Fulfillment to the Requirements

for the Award of the Degree of Master of Sciences

in Mechanical Engineering

2022

to my dear mother

ABSTRACT

A DUMMY HEAD AND NECK MODEL FOR BOTH FRONTAL AND REAR IMPACTS

YASİN DEMİRER

Master of Science, Department of Mechanical Engineering

Supervisor: Assist.Prof.Dr. Selçuk Himmetoğlu

August 2022, 70 pages

Dummies are calibrated test instruments used to measure human injury potential and determine dynamic behaviour of anatomical parts of the human in vehicle crashes. There are seperate dummies available for frontal and rear impacts.The problem is that rear impact dummies couldn't be used for frontal ones and vice versa.In this work, a multi body dummy head-neck model which could be used for rear impacts as well as frontal impacts was developed. To maintain its posture at rest, static equilibrium equations were defined on the model. The model was validated using cadaver and volunteer test data in the literature.

Keywords: rear impact, frontal impact, crash test dummy, multi-body dynamics

ÖZET

ÖNDEN VE ARKADAN ÇARPIŞMALAR İÇİN BİR MANKEN KAFA-BOYUN MODELİ

YASİN DEMİRER

Yüksek Lisans, Makina Mühendisliği Bölümü

Tez Danışmanı: Dr. Öğr. Üyesi Selçuk Himmetoğlu

Ağustos 2022, 70 sayfa

Mankenler, araç çarpışmalarında insan yaralanma potansiyelini ölçmek ve insanın anatomik bölümlerinin dinamik davranışlarını belirlemek için kullanılan kalibre edilmiş test cihazlarıdır. Önden ve arkadan çarpmalar için ayrı mankenler mevcuttur. Sorun şu ki, arkadan çarpma mankenleri önden çarpma testleri için kullanılamaz ve önden çarpma mankenleri de arkadan çarpma testleri için kullanılamaz. Bu çalışmada hem önden çarpışmalarda hem de arkadan çarpışmalarda kullanılabilecek çok cisimli bir manken kafa-boyun modeli geliştirilmiştir. Modelin duruşunu hareket etmezken koruması için model üzerinde statik denge denklemleri tanımlanmıştır. Model, literatürdeki kadavra ve gönüllü test verileri kullanılarak doğrulanmıştır.

Anahtar Kelimeler: Arkadan çarpma, önden çarpma, çarpışma test mankeni, çoklu cisim dinamiği

ACKNOWLEDGEMENTS

First and foremost, I would like to express my deepest gratitude to my supervisor Assist. Prof. Dr. Selçuk HİMMETOĞLU for his helpful suggestions, his never-ending patience and understanding, invaluable feedbacks when i needed. I sincerely thank him.

I would like to thank my Thesis Supervising Committee members for their insightful comments and suggestions

Finally, I would like to thank my family to support and encourage me during the study.

TABLE OF CONTENTS

LIST OF TABLES

LIST OF FIGURES

1.INTRODUCTION

Dummies are callibrated test devices used to measure the potential for human injury in vehicle crashes. They are produced to simulate human anatomy and biomechanical behaviour. Design of these instruments should be as simple as possible since they are used continuously and thereby it is easy to modify if any change or calibration needed.

Figure 1. RID II dummy(foreground) and HYBRID III dummy (background) [27]

Figure 2. A Test setup for BIORID II DUMMY [27]

1.1 Problem Definition

There are seperate dummies for frontal and rear impacts in crash tests. The problem is that since we can't use frontal ones for rear impacts or rear ones for frontal impacts, we need a dummy that can represent both cases.

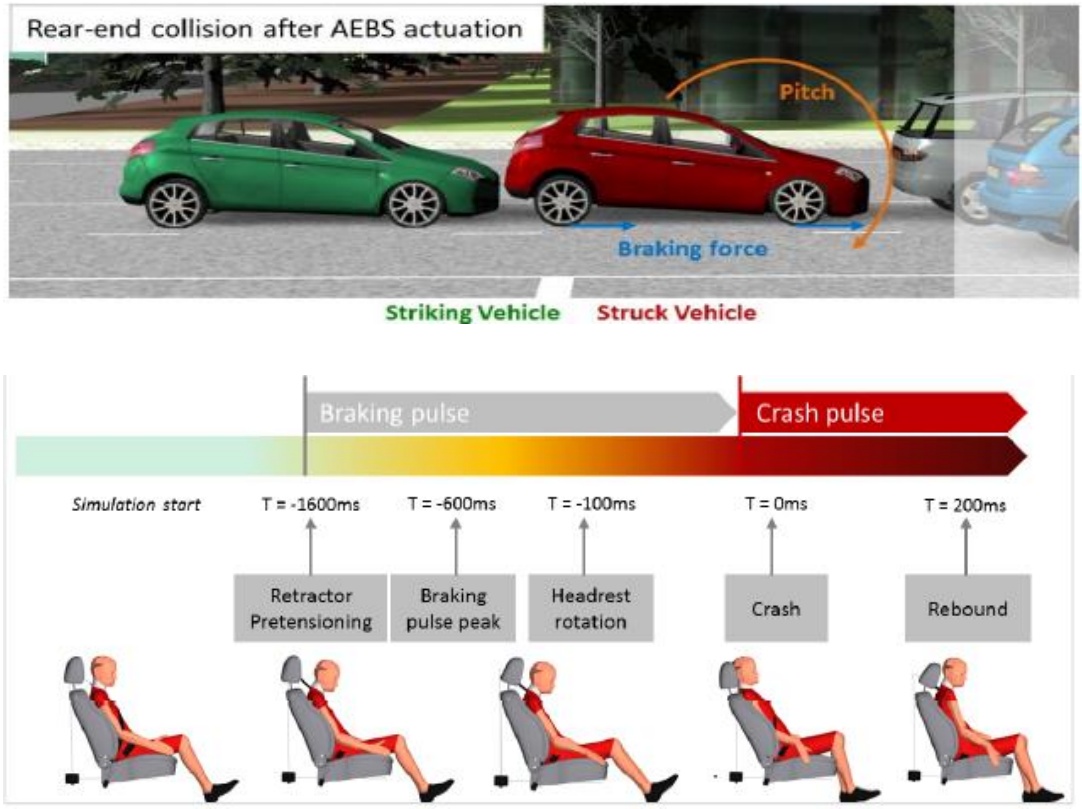

Figure 3. A traffic scenario and sequence of events for the occupant[13]

Here is another example of why we need a dummy for both frontal and rear impacts.

In Figure 3. Automatic emergency braking (AEB) system is activated when the red car approaches the gray automobile after that the green car hits the red one from the rear, therefore frontal and rear crashes could happen one after another. This is like a rebound motion for the occupant. Once such cases occur, dummies utilized for only frontal or rear crashes couldn't help us to determine the effects of the motion on the human body.

1.2 Head Neck Anatomy

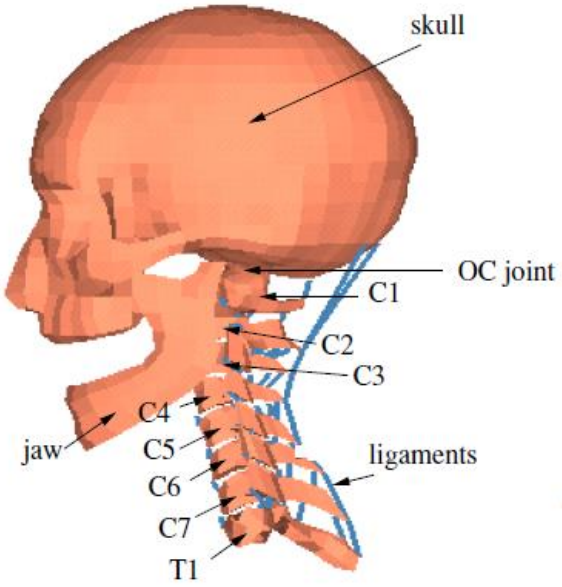

Figure 4. Head/Neck anatomy of human [1]

Human spine is made up of five spine sections. Cervical vertebrae, upper part of the spine, numbered from C1 through C7, thoracic vertebrae comprising T1 to T12, lumbar vertebrae(L1-L5), sacrum having five fused vertebrae and coccyx containing four fused vertebrae. [2]

Cervical spine, which is interest of this work, consists of 7 segments named C1 to C7. First two elements of this section, i.e, C1 and C2 also known as atlas and axis respectively, differ from each other. However, lower five vertebrae could be said roughly same in terms of geometry or shape. [2]

Between vertebrae there are soft tissues such as ligaments, intervertebral disks, facet joints and muscles surrounding them.

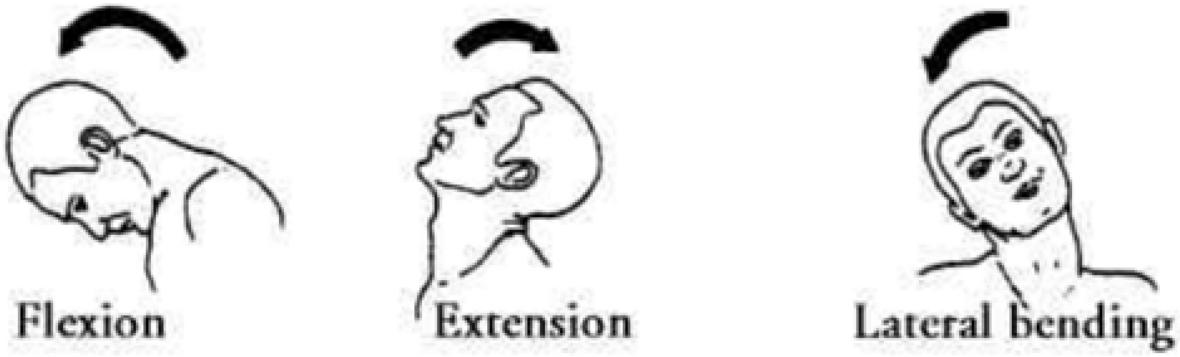

Figure 5. Terms of Head-Neck motion (Adapted from [26])

Fig.5 describes head neck motions. Flexion is the rotating of head neck to the front, while extension means rotation to the backwards. Flexion and extension occur in sagittal plane. In lateral move, head-neck is bended to the right or to the left.

2.LITERATURE SURVEY

Dummies could be classified as real dummies, finite element model dummies and multi-body model dummies.

2.1 Real Dummies

Real dummies are manufactured mechanic instruments used in crash tests. Real dummies could be summed up as rear impact dummies and frontal impact dummies.

While THOR dummies and HYBRID III dummies designed and produced for only frontal impacts, BIORID-II dummies named also ATD (Anthropometric Test Device) used for only rear impact tests.

Figure 6. THOR dummy [24]

2.2 Finite Element Dummy Models

Finite Element Models are more detailed models than other mathematical models. In these models, hard tissues such as vertebrae, bones and soft tissues such as ligaments designed as single one or two dimensional elements. While these models are good at giving elaborated information regarding tissue deformation and injury estimation , they necessitate many calculations [15] and too much time which is inefficient to make optimization on the model.

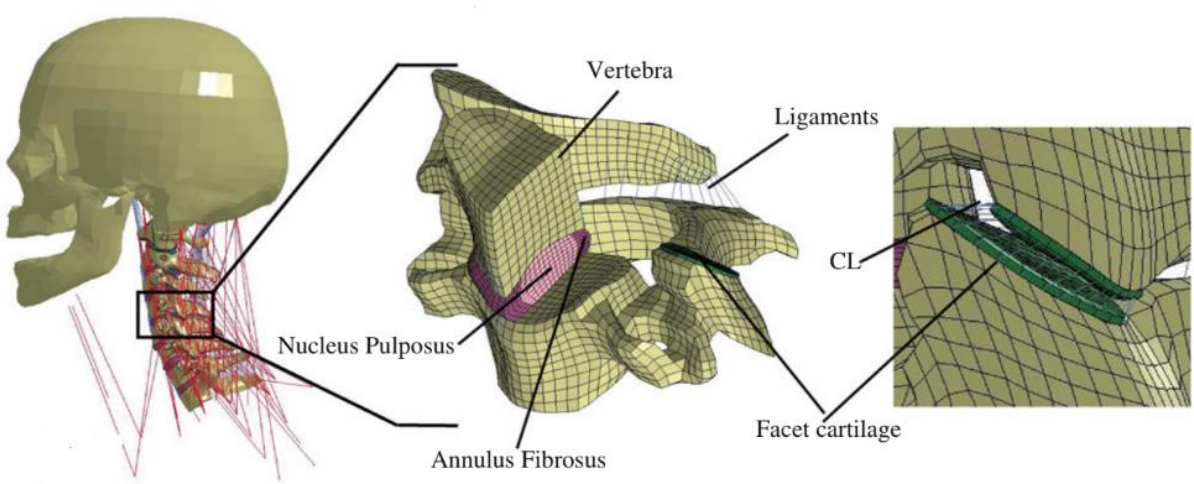

Figure 7. A finite element head and neck model[16]

There are some finite element models in the literature. Detailed information is given on the references ([17],[18],[19],[20],[21])

2.3 Multi Body Dummy Models

Multi-Body dummy models can be classified into detailed models and lumped models. In lumped models all biofidelic behaviour of head- neck is combined at intervertebral joints. Detailed models are also multi-body models including muscle elements to head neck spine. More information may be find at these references ([10],[1],[2],[12],[7])

One of the most recent multi body dummy models is that of Huang et al. Based on Anthropometric Test Device (ATD), in this work, it is designed a head and neck computer model behaving more human-like by fullfilling S-shape phenomenon which is the cause the probability of whiplash during rear impacts. Effect of soft tissues during the motion added as well. The results show that good alignment with volunteer tests [15]. However, severity of peak accelerations employed to validate the model is approximately at around 4g, which might not be appropriate for high severe rear impacts.

Multi-body model of Hoover, J. is another up to date research in the field. It is aimed that joint positions are located at instantaneous axis of rotations of vertabrae to mimic biofidelic response of head-neck spine. Lagrangian equations were utilized to obtain whiplash-like reply for available crash pulse. This model is also a lumped parameter model in which rotational springs and dampers comprising joints. Researcher makes use of inverse analysis to obtain linear stiffness and damper parameters using cadaver test data. Four model is introduced in this study to see how existence or absence of stiffness, unifrom stiffness and damping effect the responses individually. The model achieved shows reasonable results with cadaver tests [6]

Being an example of old models, De Jager developed three progressive model. In his first model, which is known as ‘global model’, a basic model with limited anatomical characteristics was created. It is composed of a rigid head and a rigid vertebrae attached by three dimensional viscoelastic elements which describe lumped mechanical behaviour of soft tissues. In his second model, cervical spine is divided into two parts:

upper and lower vertebrae where these parts are designed elaborately. Last model, which is known as ‘detailed model’, was formed by putting on muscle elements to previously created model segments. [2]

Among models in the literature, model of Van Der Horst, a novel form of de Jager’s detailed model [1], is somewhat different since it is a multi-directional model with frontal, rear and lateral validation. In his study, frontal and lateral impact test data simulated with his head-neck model. When it comes to the rear impact, whole human body was tried to validate although the responses are not good enough to the author [1]

There are some former multi-body models accessible on these references, as well. ([8],[9],[11])

3.MODEL DEVELOPMENT

The multi body model consists of a head named C0, seven neck components C1 to C7 and a body representing torso i.e, T1

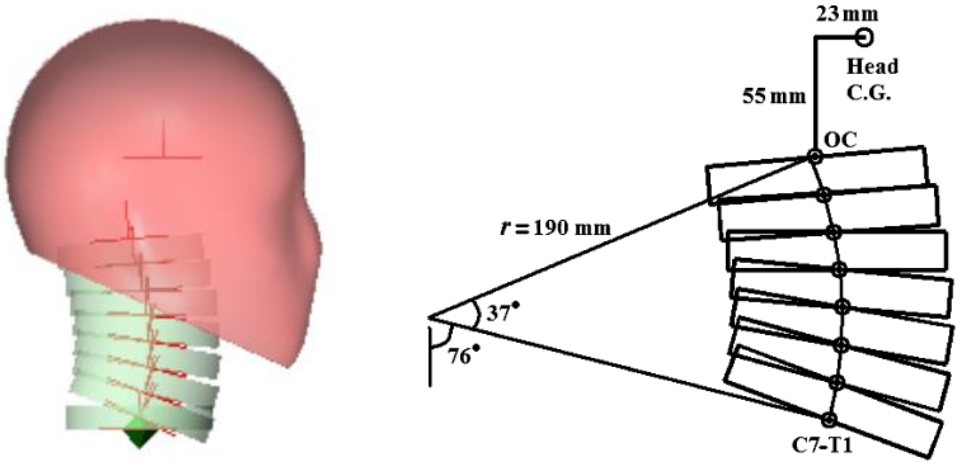

Figure 8. Head and Neck Model

		Principal moments of inertia(kg.cm^2)			Relative Orientation(deg)	
Body	Mass(kg)	I_{xx}	I_{yy}	I_{zz}	Human Neck	Multi Body Neck
C0	4.6	180	240	221	0	5
C1	0.22	2.2	2.2	4.2	0	-1.2
C2	0.25	2.5	2.5	4.8	0	-3.8
C3	0.24	2.4	2.4	4.6	-5.3	-5.3
C4	0.23	2.3	2.3	4.4	-4.7	-4.7
C5	0.23	2.3	2.3	4.5	-5.2	-5.2
C6	0.24	2.4	2.4	4.7	-5.6	-5.6
C7	0.22	2.2	2.2	4.3	20.8	20.8
T1	-	-	-	-	0	0

Table 1. Initial configuration, geometrical and inertial properties of head and neck model for 50th percentile male [2]

Neck parts have identical shape and embody the vertebrae C1 to C7. The inertial properties of each neck segments represent the equivalent mass and moments of inertia of the vertebra and the surrounding soft tissues. Geometry, initial configuration and inertial properties of the model designed for the 50th percentile male.

Between vertabrae rotational stiffness and damping coefficients are used. For all intervertebral joints same stiffness and same damping properties are applied.

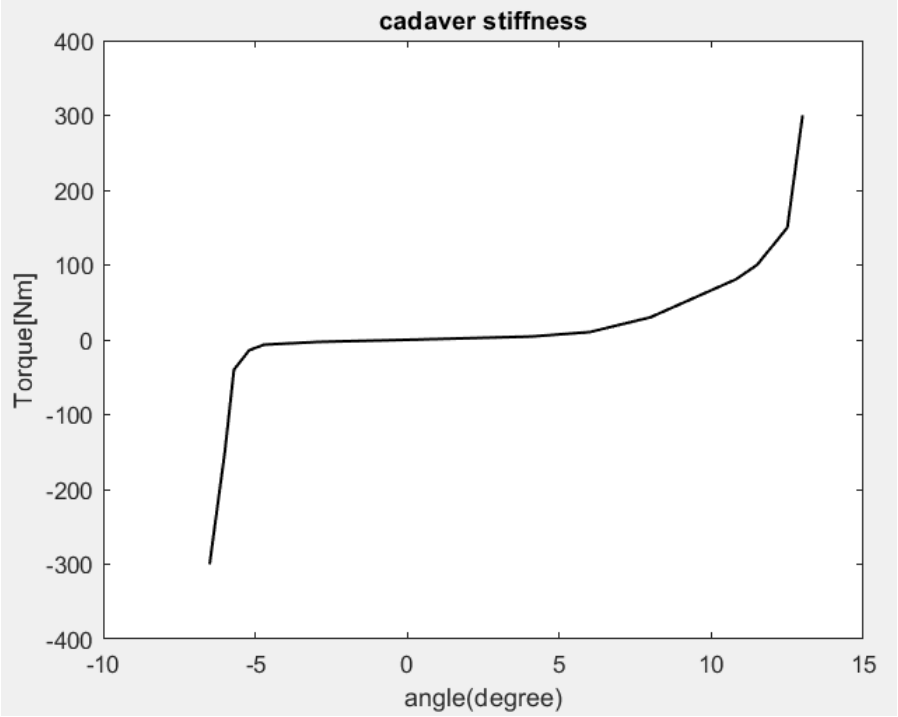

Figure 9. Rotational stiffness of intervertabral joints. Adapted from [8]

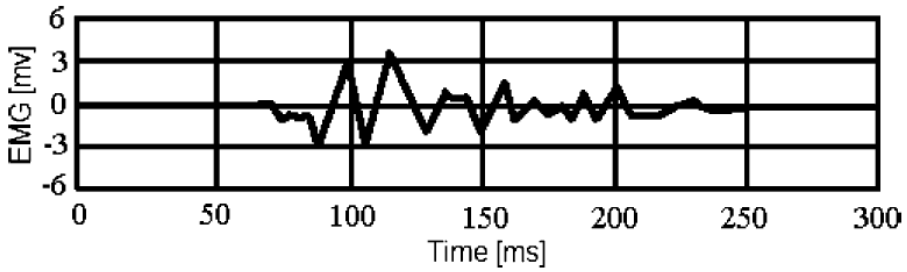

Figure 10. EMG signal of SCM muscles in Jari experiments (Taken from [14])

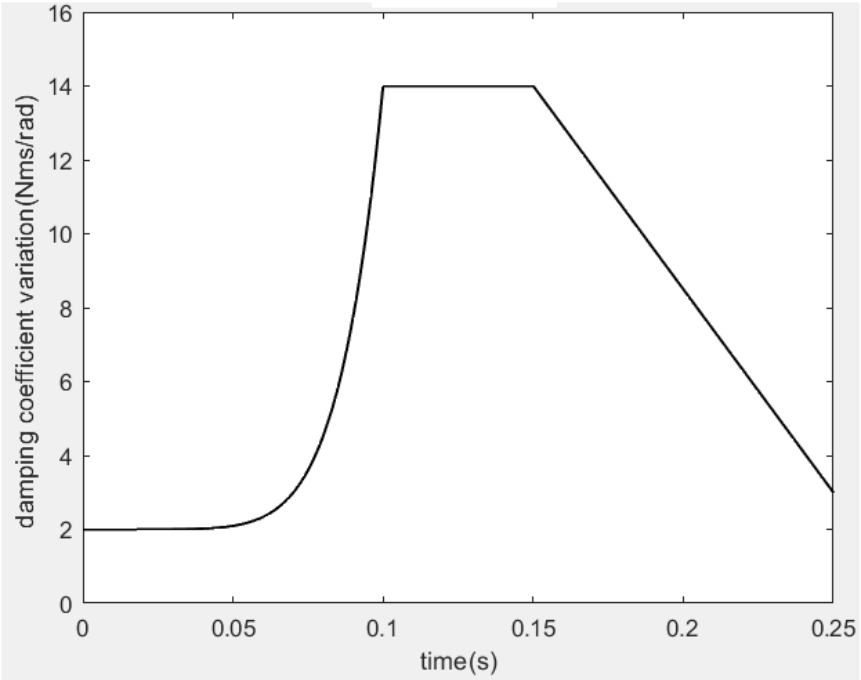

Figure 11. Damping coefficient variation (Adapted from [14])

Fig. 9 shows a non-linear rotational spring function determined with the help of cadaver experiments. It is employed on the model. However, this function does not embody muscle contraction.

In fig.10 Electromyography (EMG) signal response of the sternocleidomastoid muscle (SCM) for volunteers, which is a dominant muscle in JARI (Japanese Automobile Research Institute) experiments, is displayed. In fig.11 damping coefficient variation is created inspiring the EMG signal by the researcher [14]. For cadaver experiments since there is no active muscle response using this function on Fig.11 damping coefficient is taken 4 Nms/rad.

4. CRASH TESTS

Cadavers are dead people used for crash tests to see how they response to impacts. In cadaver tests they are equipped with accelerometers and special tools not to move just before the collision. Cadavers are of limited muscle effect and it is a good way to determine how cervical spine with soft tissues and passive muscles behave. Cadavers are examined and prepared beforehand to minimize the possible injury during the impact.

Volunteer tests are conducted to obtain how a live person response to impacts. In these tests, a volunteer attached accelerometer on its body sit down on a sled moves a direction to which the crash is applied and a pulse is created deaccelerating of the sled. There are frontal, rear and lateral impact tests available in the literature.

In this work, a cadaver test data for rear impacts, a volunteer test series for rear impacts and a volunteer test for frontal impacts are employed. Detailed information will be given in the validation part.

5.MODEL VALIDATION

5.1 Cadaver Tests

Eight cadavers not mummified were exposed to pendulum hits on the back at T1 and at T6 high severe impacts and low severe impacts having magnitude of 6.6 m/s and 4.4 m/s, respectively. They were 62 years old with a standart deviation of 12, weighed 69 kg with a standart deviation of 17 and their height was 173 cm with a standart deviation of 6.[5]

A pendulum having 23.4 kg was hanged freely by guide wires accelerated to collision speeds by a pneumatic system. Each specimen is subjected to a variety of tests: a low severe impact at T1 and T6 were conducted. Afterwards, high severe impact at T1 were performed. The cadavers were examined between tests whether they are in good condition or not.[5]

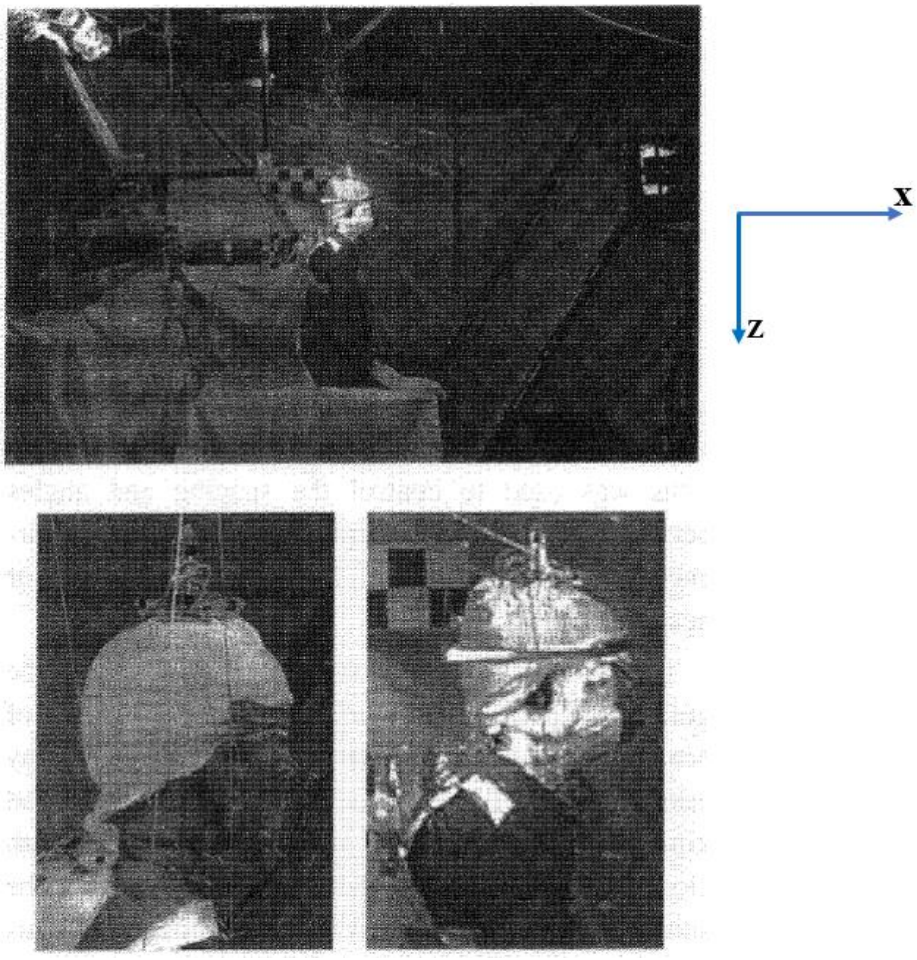

Figure 12. Tests setup and postures of cadavers before the impacts were performed [5]

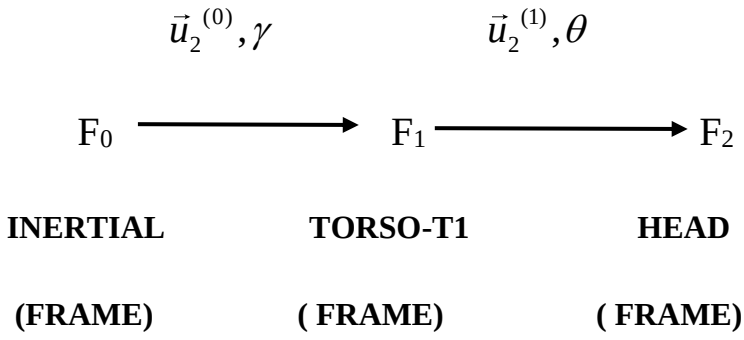

$$\phi = \gamma + \theta$$

$$H: \ Head \quad T: Torso \ or \ T1 \quad G: Ground (Inertial \ Frame)$$

$\phi = Rotation\ angle\ from\ inertial(0)\ frame\ to\ head(2)\ frame$

$\theta = Rotation\ angle\ from\ torso(1)\ frame\ to\ head(2)\ frame$

$\gamma = Rotation\ angle\ from\ inertial(0)\ frame\ to\ torso(1)\ frame$

$u_1 \to x\ ,\ u_2 \to y\ \ and\ \ u_3 \to z$

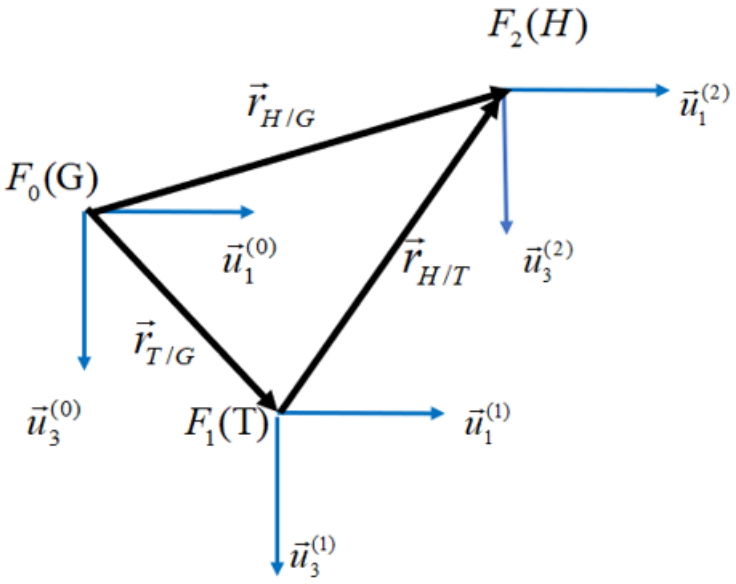

Figure 13 . Head Torso and Ground Frames used to determine orientations and displacements of torso relative to inertial (ground) frame

From the cadaver experiments head displacements relative to inertial frame, head to torso displacements given in the torso frame, and orientations of head relative to inertial frame and orientation of head with respect to torso frame which is expressed in torso frame are already available in the literature.

Using kinematic expressions between head torso and ground frames, torso,i.e. T1 vertebra displacements and orientations with respect to ground are obtained at both high T1 and at low T6 impacts.

H: Head T:Torso or T1 G:Ground Frame or Inertial Frame

Explanation of vectors and symbols used are given as follows:

$\vec{r}_{H/G}$: *Position vector of head cg frame with respect to inertial frame*

$\vec{r}_{T/G}$: *Position vector of Torso*($T1$) *frame with respect to inertial frame*

$\vec{r}_{H/T}$: *Position vector of head cg frame with respect to Torso*($T1$) *frame*

$\vec{r}_{T/G}{}^{(0)}$: *Position vector of Torso*($T1$) *frame with respect to inertial frame* (exp*ressed in inertial frame*)

γ : *Rotation angle from inertial frame*($F_{(0)}$) *to torso frame*($F_{(1)}$)

X : *Position of head w.r.t inertial frame in* $x(\vec{u}_1^{(0)})$ *direction* (exp*ressed in inertial frame*)

Z : *Position of head w.r.t inertial frame in* $z(\vec{u}_3^{(0)})$ *direction* (exp*ressed in inertial frame*)

$X-T$: *Position of head w.r.t. torso frame in* $x(\vec{u}_1^{(1)})$ *direction* (exp*ressed in torso frame*)

$Z-T$: *Position of head w.r.t. torso frame in* $z(\vec{u}_3^{(1)})$ *direction* (exp*ressed in torso frame*)

$(X-T)_i$: Initial position of head w.r.t. torso frame in $x(\vec{u}_1^{(1)})$ *direction*

$(\mathrm{Z}-T)_i$: Initial position of head w.r.t. torso frame in $z(\vec{u}_3^{(1)})$ *direction*

$C^{(0,1)}$ = *rotation matrix from inertial frame*($F_{(0)}$) *to torso*($F_{(1)}$) *frame*

Head frame and inertial frame are coincident at initial time

Displacement vector expressions between head, torso and ground frames for both High-severe T1 impact and Low-severe T6 impact are as follows:

$$\vec{r}_{H/G} = \vec{r}_{\mathrm{T}/G} + \vec{r}_{H/\mathrm{T}} \qquad \vec{r}_{\mathrm{T}/G} = \vec{r}_{H/G} - \vec{r}_{H/\mathrm{T}}$$

$$\vec{r}_{\mathrm{T}/G} = X\,\vec{u}_1^{(0)} + Z\,\vec{u}_3^{(0)} - [(\mathrm{X}-\mathrm{T}+(\mathrm{X}-\mathrm{T})_i)\vec{u}_1^{(1)} + (\mathrm{Z}-\mathrm{T}-(\mathrm{Z}-\mathrm{T})_i)\vec{u}_3^{(1)}]$$

in inertial frame we get $\vec{r}_{\mathrm{T}/G}{}^{(0)}$ *as* exp*ressed below*

$$\vec{r}_{\mathrm{T}/G}{}^{(0)} = X\,\vec{u}_1^{(0)} + Z\,\vec{u}_3^{(0)} - C^{(0,1)}(\mathrm{X}-\mathrm{T}+(\mathrm{X}-\mathrm{T})_i)\vec{u}_1^{(1/0)} - C^{(0,1)}(\mathrm{Z}-\mathrm{T}-(\mathrm{Z}-\mathrm{T})_i)\vec{u}_3^{(1/0)}$$

$$C^{(0,1)} = e^{\tilde{u}_2\gamma}\,,\ e^{\tilde{u}_2\gamma}\vec{u}_1^{(1/0)} = \vec{u}_1^{(0)}\cos\gamma - \vec{u}_3^{(0)}\sin\gamma \quad \textit{and}$$
$$e^{\tilde{u}_2\gamma}\vec{u}_3^{(1/0)} = \vec{u}_3^{(0)}\cos\gamma + \vec{u}_1^{(0)}\sin\gamma$$

$$\vec{r}_{\mathrm{T}/G}{}^{(0)} = X\,\vec{u}_1^{(0)} + Z\,\vec{u}_3^{(0)} - (\vec{u}_1^{(0)}\cos\gamma - \vec{u}_3^{(0)}\sin\gamma)(\mathrm{X}-\mathrm{T}+(\mathrm{X}-\mathrm{T})_i) - (\vec{u}_3^{(0)}\cos\gamma + \vec{u}_1^{(0)}\sin\gamma)(\mathrm{Z}-\mathrm{T}-(\mathrm{Z}-\mathrm{T})_i)$$

$$\vec{r}_{\mathrm{T}/G}{}^{(0)} = [\mathrm{X}-\cos\gamma(\mathrm{X}-\mathrm{T}+(\mathrm{X}-\mathrm{T})_i) - \sin\gamma(\mathrm{Z}-\mathrm{T}-(\mathrm{Z}-\mathrm{T})_i)]\vec{u}_1^{(0)} + [\mathrm{Z}+\sin\gamma(\mathrm{X}-\mathrm{T}+(\mathrm{X}-\mathrm{T})_i) - \cos\gamma(\mathrm{Z}-\mathrm{T}-(\mathrm{Z}-\mathrm{T})_i)]\vec{u}_3^{(0)} \quad .....(1)$$

$$(\mathrm{X}-\mathrm{T})_i = (X_T)_i \qquad (\mathrm{Z}-\mathrm{T})_i = (\mathrm{Z}_T)_i$$

5.1.1 Role of Initial Conditions

There is not any information about the initial conditions of cadaver experiments. Whether the terms $(\mathrm{X}_T)_i$ and $(\mathrm{Z}_T)_i$,which means initial conditions of head cg with respect to torso, must be included or not included in the equation (1) should be clarified since our aim is to give the acceleration of torso relative to inertial frame (expressed in inertial frame) as input on the back at T1 in the model designed in Msc Visual Nastran 4D. Taking first and second derivative of equation (1)

$$\begin{aligned}\vec{\dot{r}}_{T/G}{}^{(0)} = [&\dot{X} + \sin\gamma\,\dot{\gamma}(\mathrm{X}_T + (\mathrm{X}_T)_i) - (\dot{\mathrm{X}}_T + (\dot{\mathrm{X}}_T)_i)\cos\gamma - \cos\gamma\,\dot{\gamma}(Z_T - (Z_T)_i) \\ &- \sin\gamma(\dot{Z}_T - (\dot{Z}_T)_i)]\vec{u}_1{}^0 + [\dot{Z} + \cos\gamma\,\dot{\gamma}(\mathrm{X}_T + (\mathrm{X}_T)_i) + (\dot{\mathrm{X}}_T + (\dot{\mathrm{X}}_T)_i)\sin\gamma \\ &+ \sin\gamma\,\dot{\gamma}(Z_T - (Z_T)_i) - \cos\gamma(\dot{Z}_T - (\dot{Z}_T)_i)]\vec{u}_3{}^0\end{aligned}$$

$$(\dot{\mathrm{X}}_T)_i = 0 \ , \ (\dot{Z}_T)_i = 0$$

$$\begin{aligned}\vec{\dot{r}}_{T/G}{}^{(0)} = [&\dot{X} + \sin\gamma\,\dot{\gamma}(\mathrm{X}_T + (\mathrm{X}_T)_i) - \dot{\mathrm{X}}_T\cos\gamma - \cos\gamma\,\dot{\gamma}(Z_T - (Z_T)_i) \\ &- \sin\gamma\,\dot{Z}_T]\vec{u}_1{}^0 + [\dot{Z} + \cos\gamma\,\dot{\gamma}(\mathrm{X}_T + (\mathrm{X}_T)_i) + \dot{\mathrm{X}}_T\sin\gamma \\ &+ \sin\gamma\,\dot{\gamma}(Z_T - (Z_T)_i) - \cos\gamma\,\dot{Z}_T]\vec{u}_3{}^0\end{aligned}$$

$$\begin{aligned}\vec{\dot{r}}_{T/G}{}^{(0)} = [&\dot{X} + \sin\gamma\,\dot{\gamma}\,\mathrm{X}_T - \dot{\mathrm{X}}_T\cos\gamma - \cos\gamma\,\dot{\gamma}Z_T - \sin\gamma\,\dot{Z}_T]\vec{u}_1{}^0 + \\ &[\dot{Z} + \cos\gamma\,\dot{\gamma}\,\mathrm{X}_T + \dot{\mathrm{X}}_T\sin\gamma + \sin\gamma\,\dot{\gamma}Z_T - \cos\gamma\,\dot{Z}_T]\vec{u}_3{}^0 + \\ &[\sin\gamma\,\dot{\gamma}(\mathrm{X}_T)_i + \cos\gamma\,\dot{\gamma}(Z_T)_i]\vec{u}_1{}^0 + [\cos\gamma\,\dot{\gamma}(\mathrm{X}_T)_i - \sin\gamma\,\dot{\gamma}(Z_T)_i]\vec{u}_3{}^0\end{aligned}$$

$$\begin{aligned}\vec{\dot{r}}_{T/G}{}^{(0)} = &(\vec{\dot{r}}_{T/G}{}^{(0)})^* + [\sin\gamma\,\dot{\gamma}(\mathrm{X}_T)_i + \cos\gamma\,\dot{\gamma}(Z_T)_i]\vec{u}_1{}^0 + \\ &[\cos\gamma\,\dot{\gamma}(\mathrm{X}_T)_i - \sin\gamma\,\dot{\gamma}(Z_T)_i]\vec{u}_3{}^0\end{aligned}$$

$\vec{\dot{r}}_{T/G}{}^{(0)} \rightarrow$ *velocity of torso with respect to inertial frame with initial conditions*

$(\vec{\dot{r}}_{T/G}{}^{(0)})^* \rightarrow$ *velocity of torso with respect to inertial frame without initial conditions*

$$\vec{\ddot{r}}_{T/G}{}^{(0)} = [\ddot{X} + (\cos\gamma(\dot{\gamma})^2 + \ddot{\gamma}\sin\gamma)(X_T + (X_T)_i) + \sin\gamma\dot{\gamma}(\dot{X}_T + (\dot{X}_T)_i) +$$
$$\sin\gamma\dot{\gamma}\dot{X}_T - \cos\gamma\ddot{X}_T + (\sin\gamma(\dot{\gamma})^2 - \cos\gamma\ddot{\gamma})(\mathrm{Z}_T - (\mathrm{Z}_T)_i) -$$
$$\cos\gamma\dot{\gamma}(\dot{\mathrm{Z}}_T - (\dot{\mathrm{Z}}_T)_i) - \cos\gamma\dot{\gamma}\dot{\mathrm{Z}}_T - \sin\gamma\ddot{\mathrm{Z}}_T]\vec{u}_1{}^0 +$$
$$[\ddot{\mathrm{Z}} + (-\sin\gamma(\dot{\gamma})^2 + \ddot{\gamma}\cos\gamma)(X_T + (X_T)_i) + \cos\gamma\dot{\gamma}(\dot{X}_T + (\dot{X}_T)_i) +$$
$$\cos\gamma\dot{\gamma}\dot{X}_T + \sin\gamma\ddot{X}_T + (\cos\gamma(\dot{\gamma})^2 + \sin\gamma\ddot{\gamma})(\mathrm{Z}_T - (\mathrm{Z}_T)_i) +$$
$$\sin\gamma\dot{\gamma}(\dot{\mathrm{Z}}_T - (\dot{\mathrm{Z}}_T)_i) + \sin\gamma\dot{\gamma}\dot{\mathrm{Z}}_T - \cos\gamma\ddot{\mathrm{Z}}_T]\vec{u}_3{}^0$$

$$(\dot{\mathrm{X}}_T)_i = 0 \ , \ (\dot{Z}_T)_i = 0$$

$$\vec{\ddot{r}}_{T/G}{}^{(0)} = [\ddot{X} + (\cos\gamma(\dot{\gamma})^2 + \ddot{\gamma}\sin\gamma)(X_T) + 2\sin\gamma\dot{\gamma}(\dot{X}_T) - \cos\gamma\ddot{\mathrm{X}}_T$$
$$+ (\sin\gamma(\dot{\gamma})^2 - \cos\gamma\ddot{\gamma})(\mathrm{Z}_T) - 2\cos\gamma\dot{\gamma}(\dot{\mathrm{Z}}_T) - \sin\gamma\ddot{\mathrm{Z}}_T]\vec{u}_1{}^0 +$$
$$[\ddot{\mathrm{Z}} + (-\sin\gamma(\dot{\gamma})^2 + \ddot{\gamma}\cos\gamma)(X_T) + 2\cos\gamma\dot{\gamma}(\dot{X}_T) + \sin\gamma\ddot{X}_T$$
$$+ (\cos\gamma(\dot{\gamma})^2 + \sin\gamma\ddot{\gamma})(\mathrm{Z}_T) + 2\sin\gamma\dot{\gamma}(\dot{\mathrm{Z}}_T) - \cos\gamma\ddot{\mathrm{Z}}_T]\vec{u}_3{}^0 +$$
$$[(\cos\gamma(\dot{\gamma})^2 + \ddot{\gamma}\sin\gamma)(X_T)_i + (\cos\gamma\ddot{\gamma} - \sin\gamma(\dot{\gamma})^2(\mathrm{Z}_T)_i]\vec{u}_1{}^0 +$$
$$[(-\sin\gamma(\dot{\gamma})^2 + \ddot{\gamma}\cos\gamma)(X_T)_i - (\cos\gamma(\dot{\gamma})^2 + \sin\gamma\ddot{\gamma})(\mathrm{Z}_T)_i]\vec{u}_3{}^0$$

$$\vec{\ddot{r}}_{T/G}{}^{(0)} = (\vec{\ddot{r}}_{T/G}{}^{(0)})^* + [(\cos\gamma(\dot{\gamma})^2 + \ddot{\gamma}\sin\gamma)(X_T)_i + (\cos\gamma\ddot{\gamma} - \sin\gamma(\dot{\gamma})^2(\mathrm{Z}_T)_i]\vec{u}_1{}^0$$
$$+ [(-\sin\gamma(\dot{\gamma})^2 + \ddot{\gamma}\cos\gamma)(X_T)_i - (\cos\gamma(\dot{\gamma})^2 + \sin\gamma\ddot{\gamma})(\mathrm{Z}_T)_i]\vec{u}_3{}^0$$

$\vec{\ddot{r}}_{T/G}{}^{(0)}$ $\rightarrow$ *acceleration of torso with respect to inertial frame with initial conditions*

$(\vec{\ddot{r}}_{T/G}{}^{(0)})^*$ $\rightarrow$ *acceleration of torso with respect to inertial frame without initial conditions*

As seen on above, initial displacements of head frame with respect to torso frame changes the acceleration input values. Therefore, initial displacements are included in the calculations and indicated on figure 14 . For simplicity, initial orientations of head frame, torso frame and initial frame taken same as zero with horizontal.

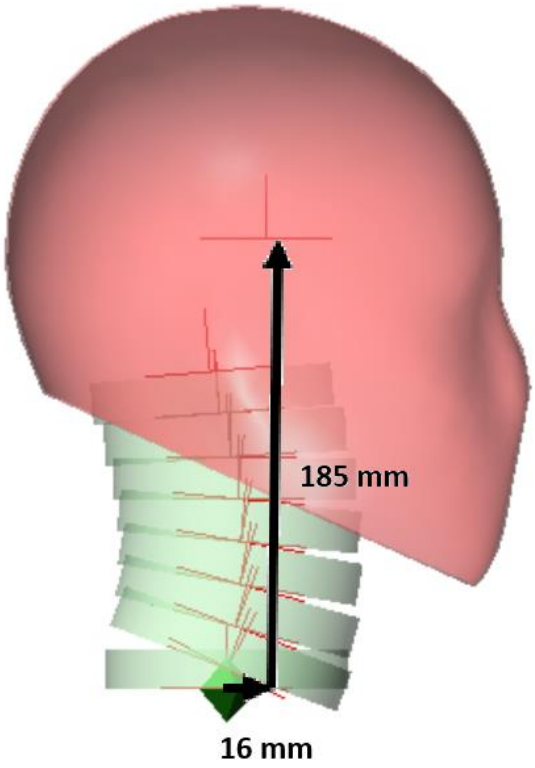

Figure 14. Initial displacements between head center of gravity and torso center of gravity of the head and neck model

Using matlab and data from literature on average cadavers and employing equation (1) we get torso experimental orientations data and experimental displacements data relative to inertial frame.

As for obtaining smoothed data (red dashed), first SAE J211 filter, which is a standart of Society of Automobile Engineers, applied on previously calculated experimental acceleration input values. Afterwards, taking numerical integration two times we can get the smoothed orientations data and smoothed displacements data.

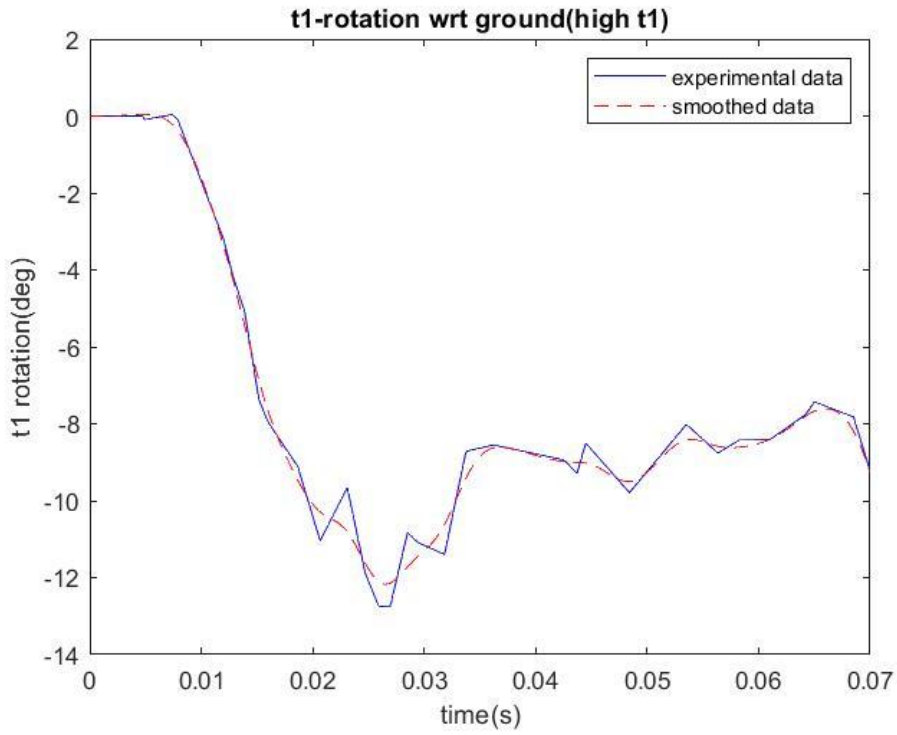

Figure 15. Experimental data obtained and smoothed data for orientation of torso relative to inertial frame on back high severe impact at T1

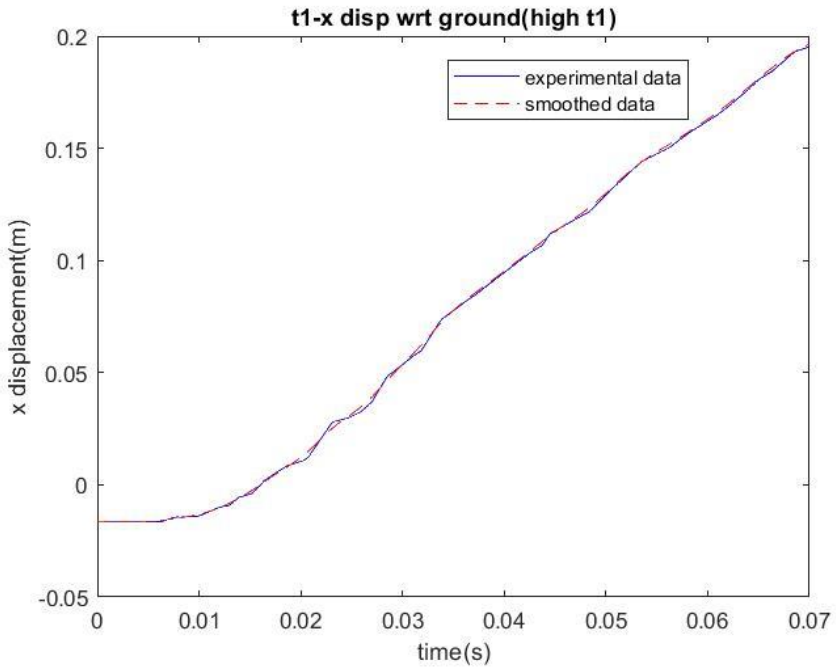

Figure 16. Experimental data obtained and smoothed data for displacement of torso relative to inertial frame in x direction on back high severe impact at T1

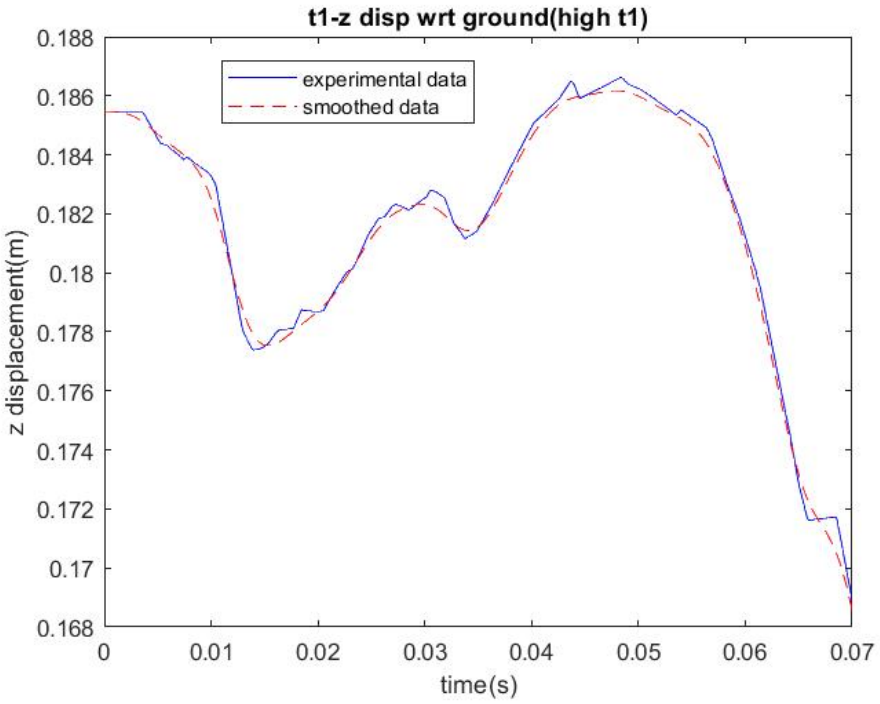

Figure 17. Experimental data obtained and smoothed data for displacement of torso relative to inertial frame in z direction on back high severe impact at T1

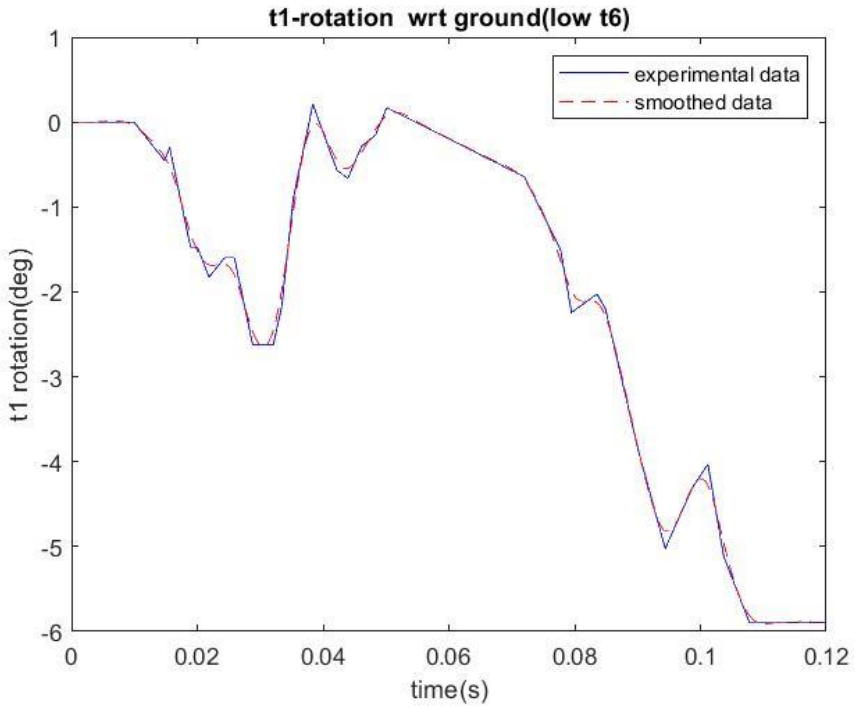

Figure 18. Experimental data obtained and smoothed data for orientation of torso relative to inertial frame on back low severe impact at T6

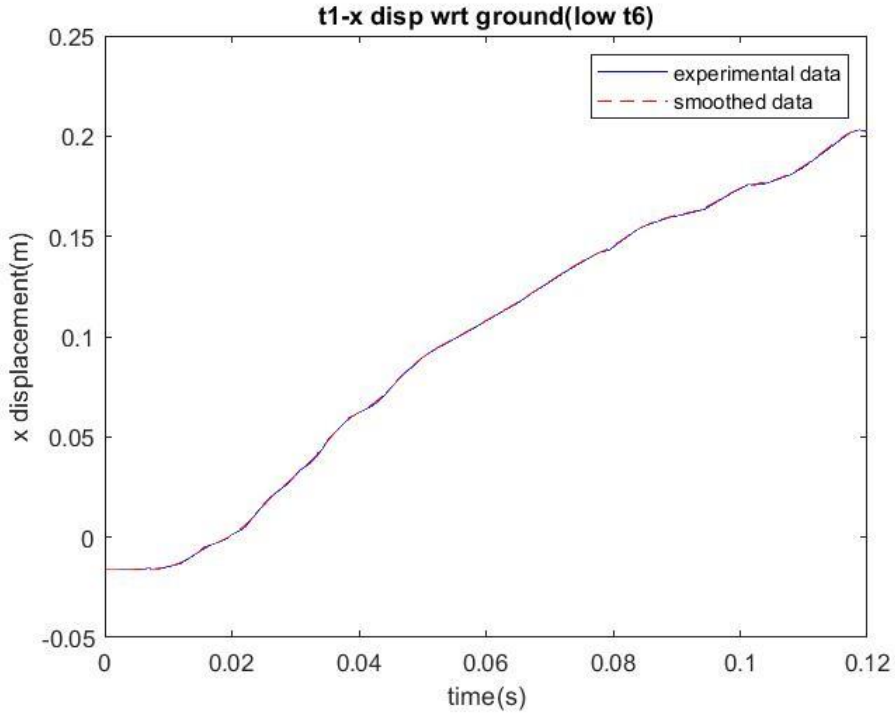

Figure 19. Experimental data obtained and smoothed data for displacement of torso relative to inertial frame in x direction on back low severe impact at T6

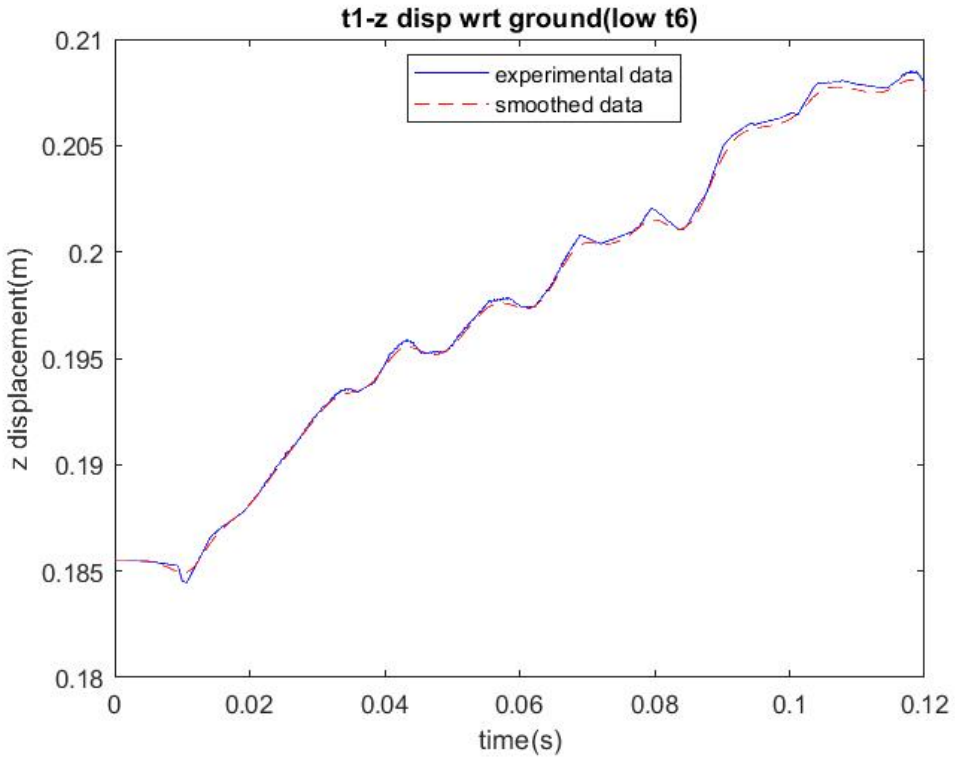

Figure 20. Experimental data obtained and smoothed data for displacement of torso relative to inertial frame in z direction on back low severe impact at T6

5.1.2 Head and Neck Model Responses with Cadaver Data (High severe impact on back at T1)

Smoothed acceleration values for high severe impact on back at T1 and low severe impact at T6 are given to the T1 on the head and neck model designed in Msc Visual Nastran 4D as input. Results obtained are compared with cadaver response corridor of the tests.

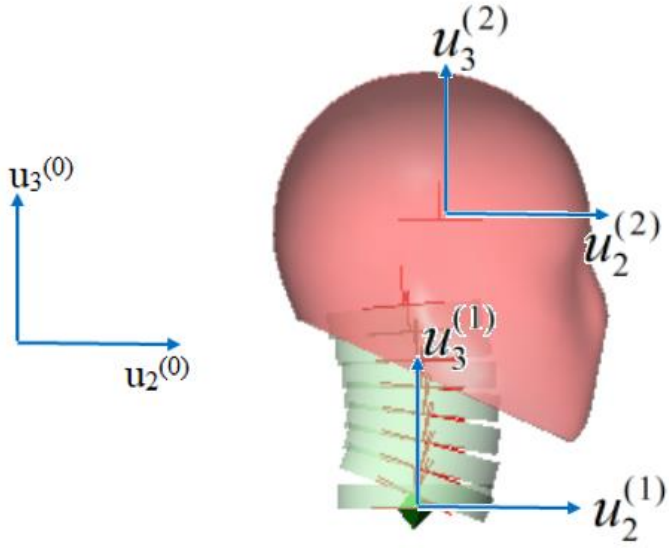

Figure 21. Frames used on the head and neck model

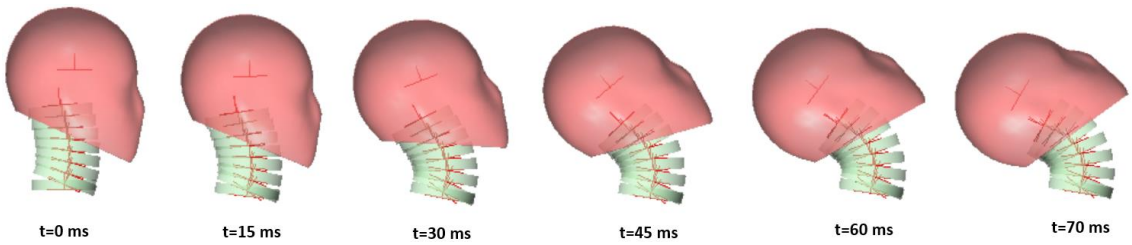

Figure 22. Time history of head neck model simulation with high severe impact on back at T1

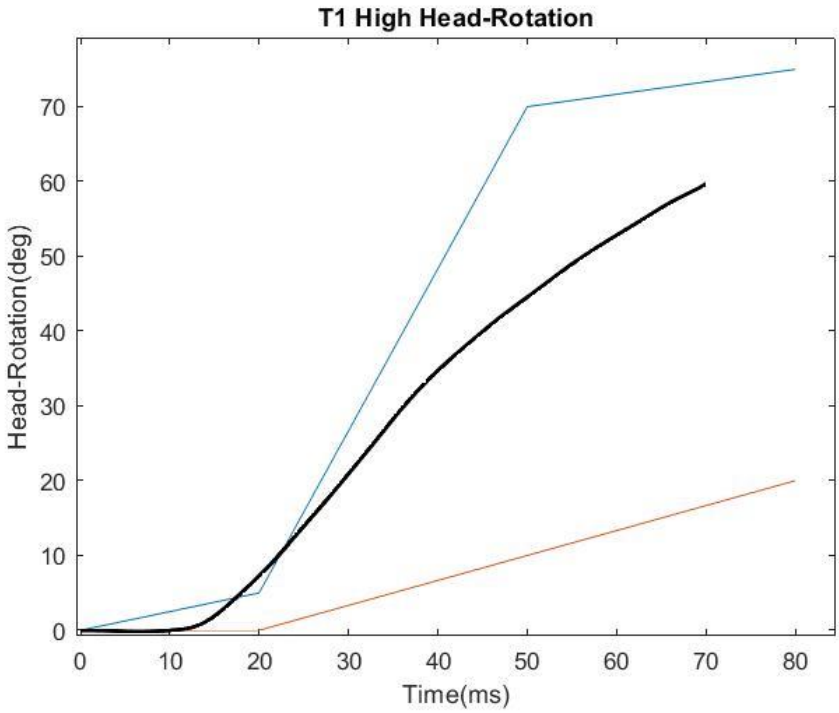

Figure 23. Orientation of head relative to inertial frame (expressed in inertial frame) on back high severe impact at T1

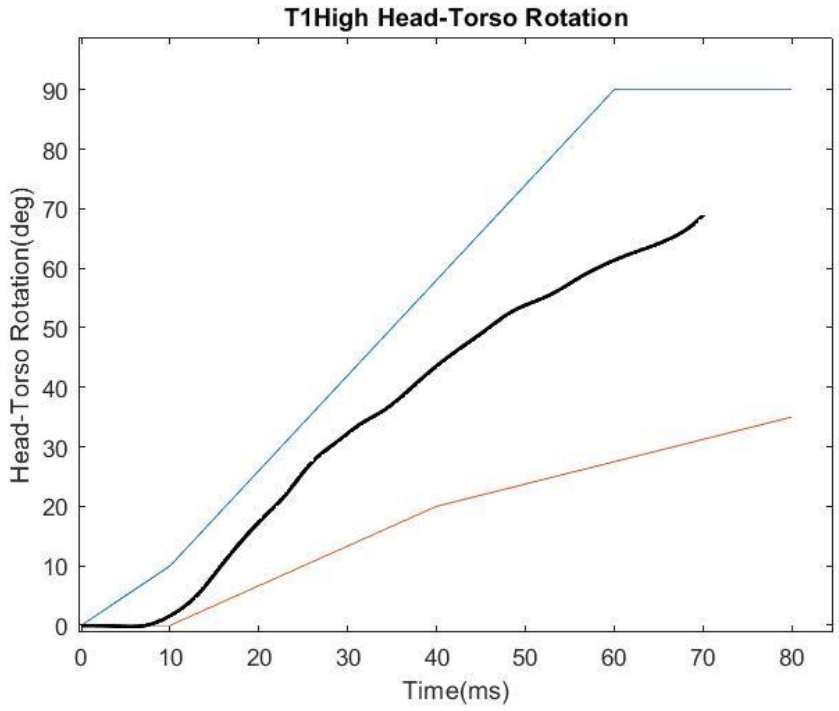

Figure 24. Orientation of Head with respect to Torso (expressed in torso frame) on back high severe impact at T1

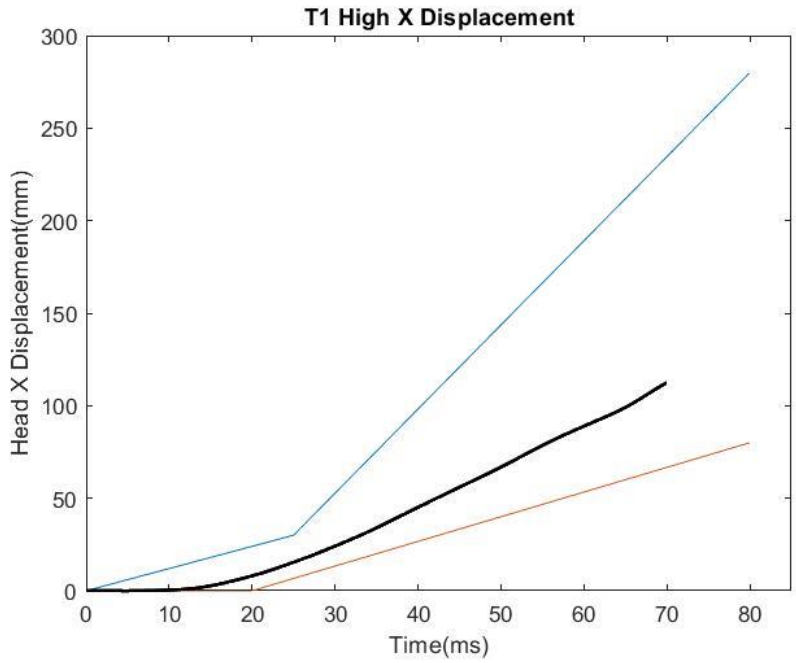

Figure 25. Head Displacement with respect to ground in x direction (expressed in ground frame) on back high severe impact at T1

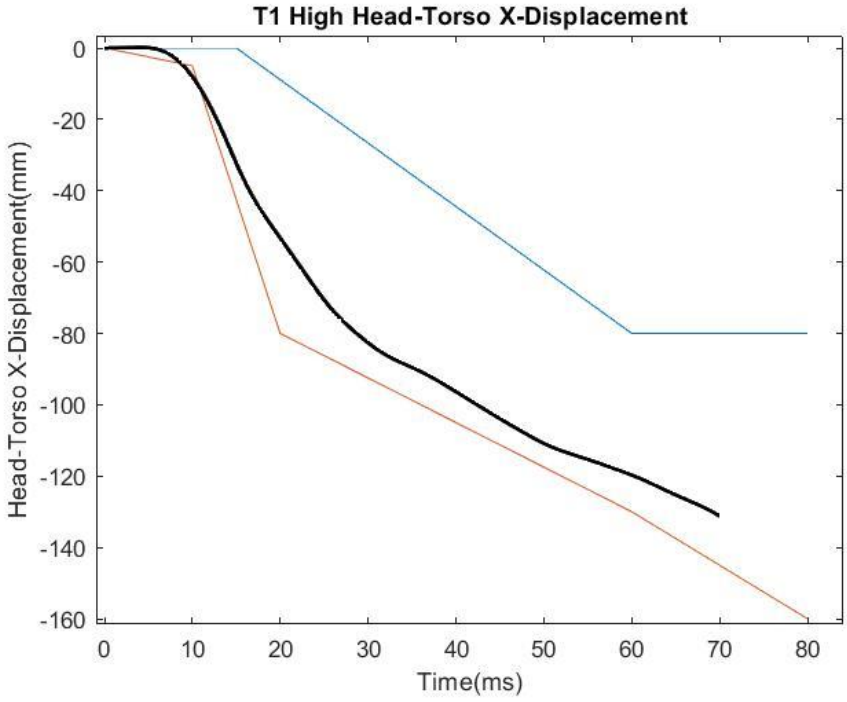

Figure 26. Head Displacement with respect to torso in x direction (expressed in torso frame) on back high severe impact at T1

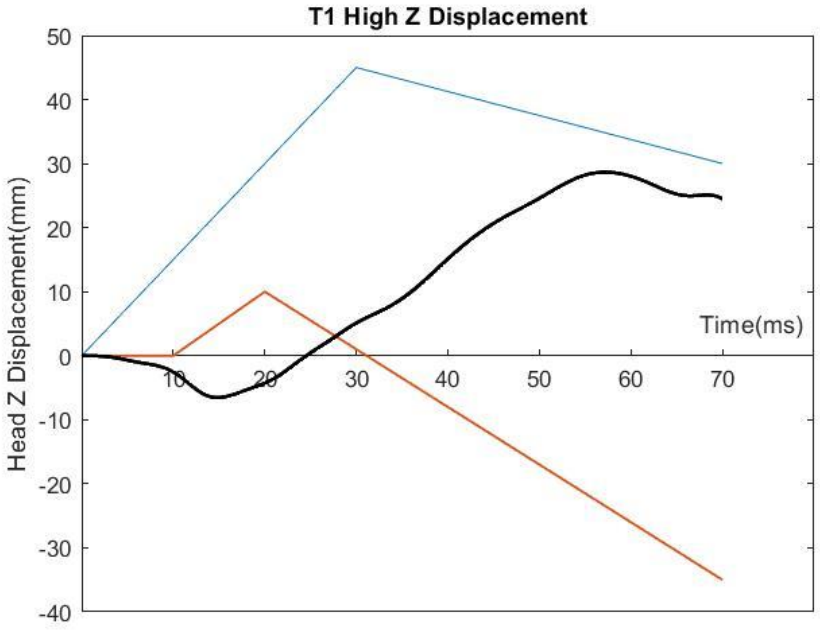

Figure 27. Head Displacement with respect to ground in z direction (expressed in ground frame) on back high severe impact at T1

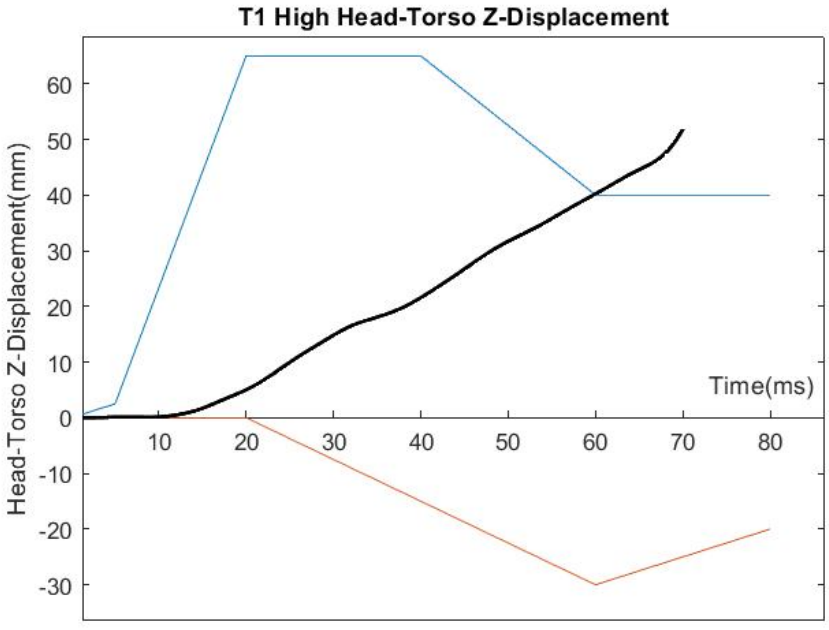

Figure 28. Head Displacement with respect to torso in z direction (expressed in torso frame) on back high severe impact at T1

5.1.3 Head and Neck Model Responses with Cadaver Data (Low severe impact on back at T6)

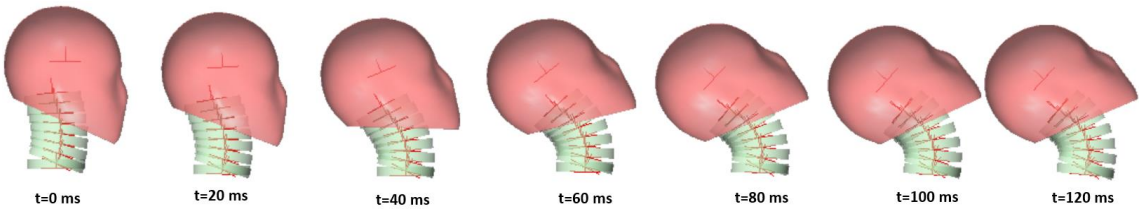

Figure 29. Time history of head neck model simulation with low severe impact on back at T6

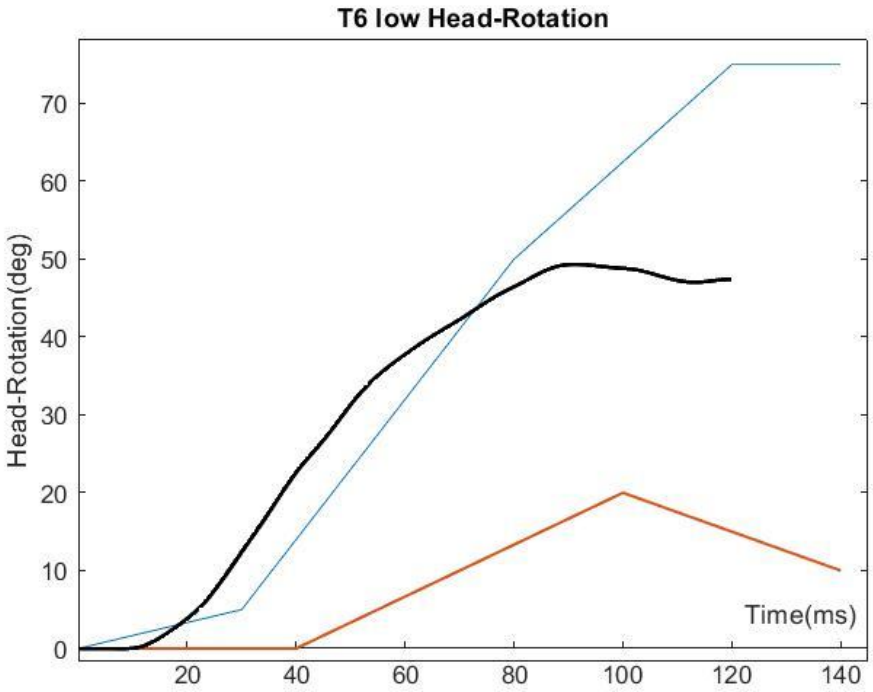

Figure 30. Orientation of head relative to inertial frame (expressed in inertial frame) on back low severe impact at T6

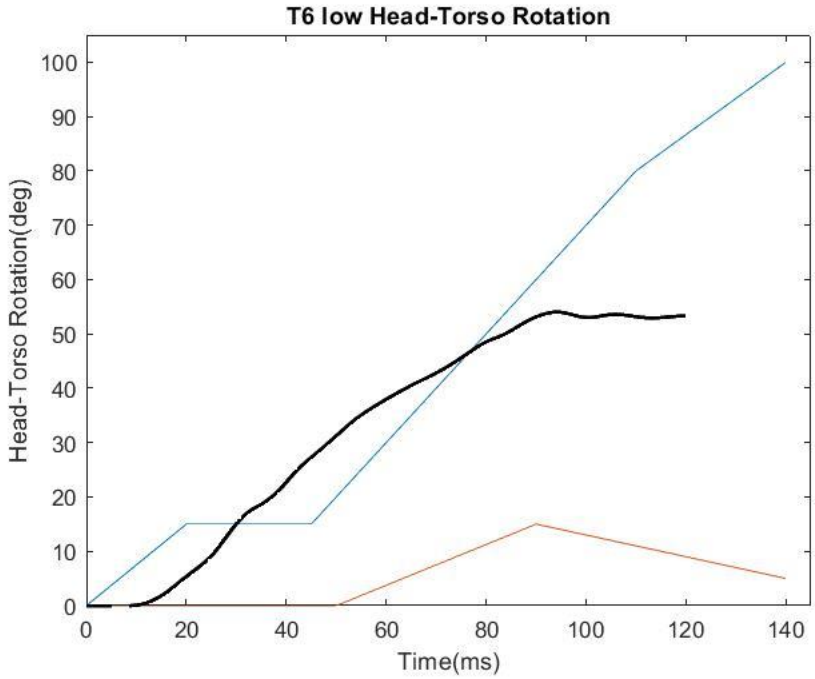

Figure 31. Orientation of head with respect to torso (expressed in torso frame) on back low severe impact at T6

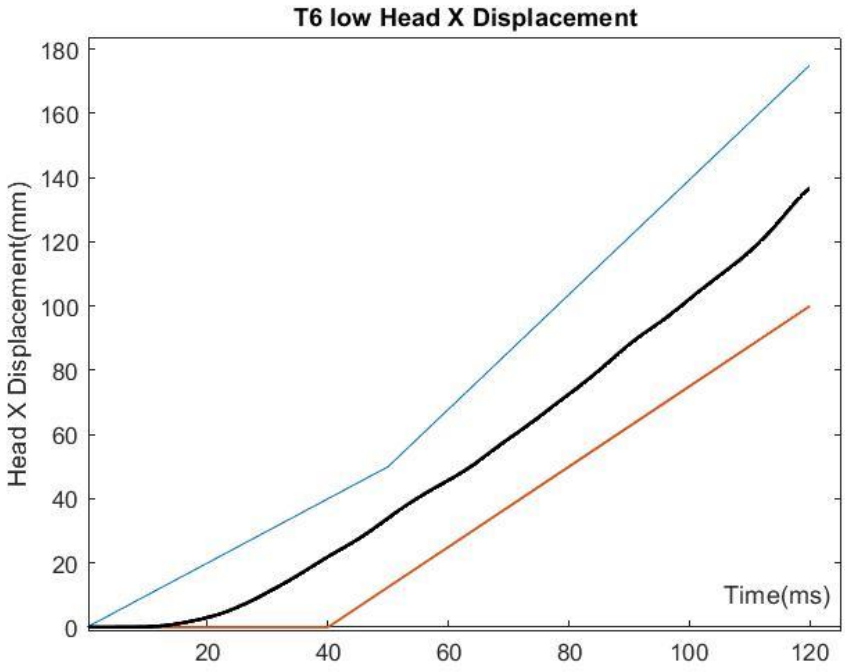

Figure 32. Head Displacement with respect to ground in x direction (expressed in ground frame) on back low severe impact at T6

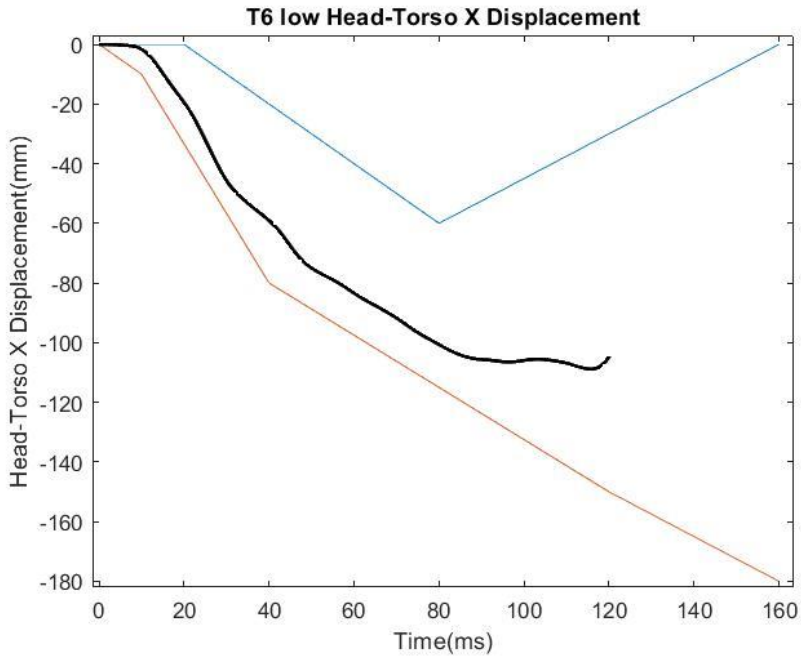

Figure 33. Head Displacement with respect to Torso in x direction (expressed in torso frame) on back low severe impact at T6

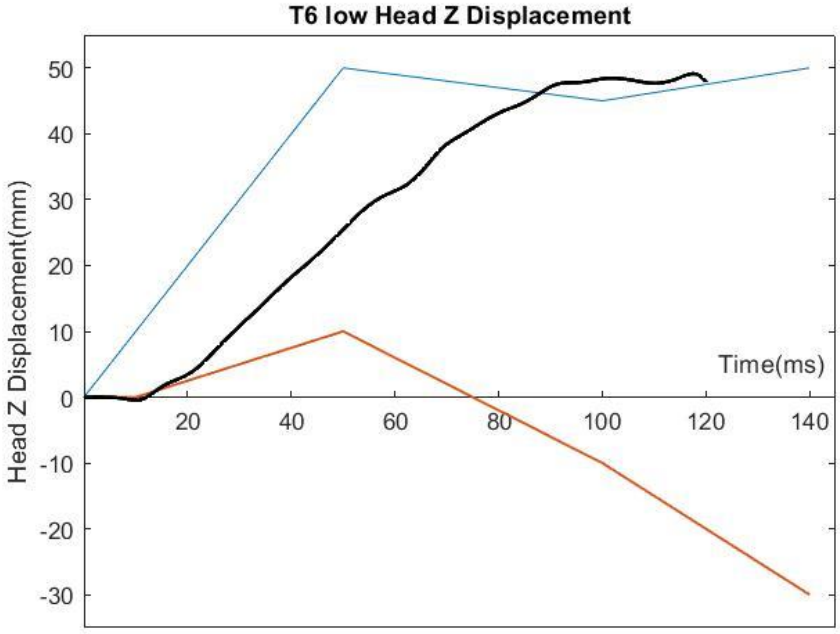

Figure 34. Head Displacement with respect to ground in z direction (expressed in ground frame) on back low severe impact at T6

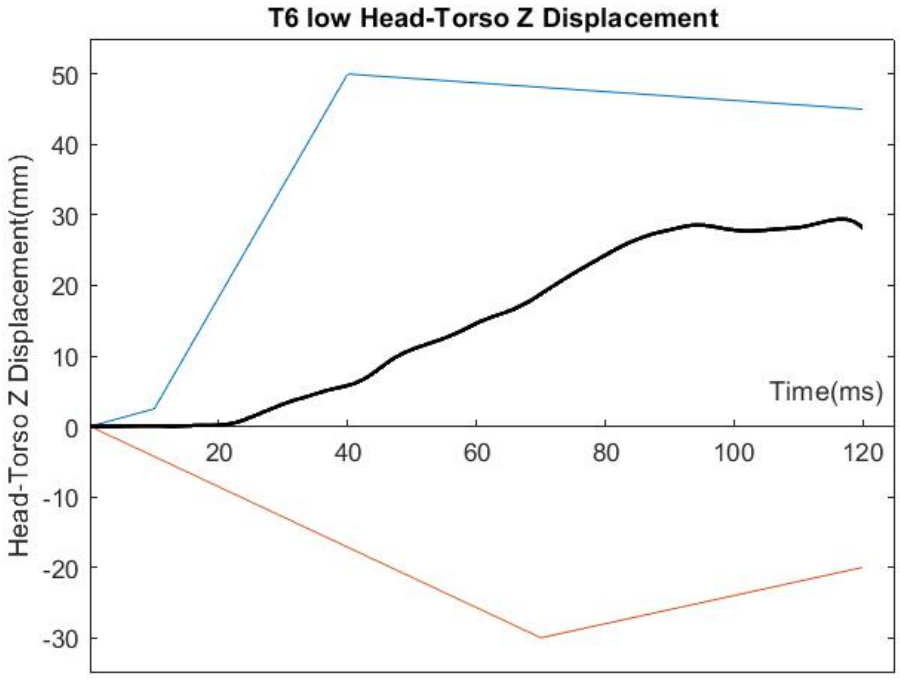

Figure 35. Head Displacement with respect to Torso in z direction (expressed in torso frame) on back low severe impact at T6

As seen in the figures head and neck model results are in good alignment with cadaver corridors.In two simulations while head rotates counterclokwise and torso(t1) rotates clockwise head torso rotations turn out more than head rotations.Furthermore, head rotations, head torso rotations and displacements in high severe impact at T1 are in general higher than those of in low severe impact at T6 since the reason is probably the impact speed which cause torso to move forward a bit more and head to rotate backwards further

5.2 HEAD NECK MODEL STATIC EQUILIBRIUM FORMULATION FOR MUSCLE TONE

Muscle tone is described as the constant and passive contraction of muscles at rest, which ensures static balance and maintains human body posture.[23]

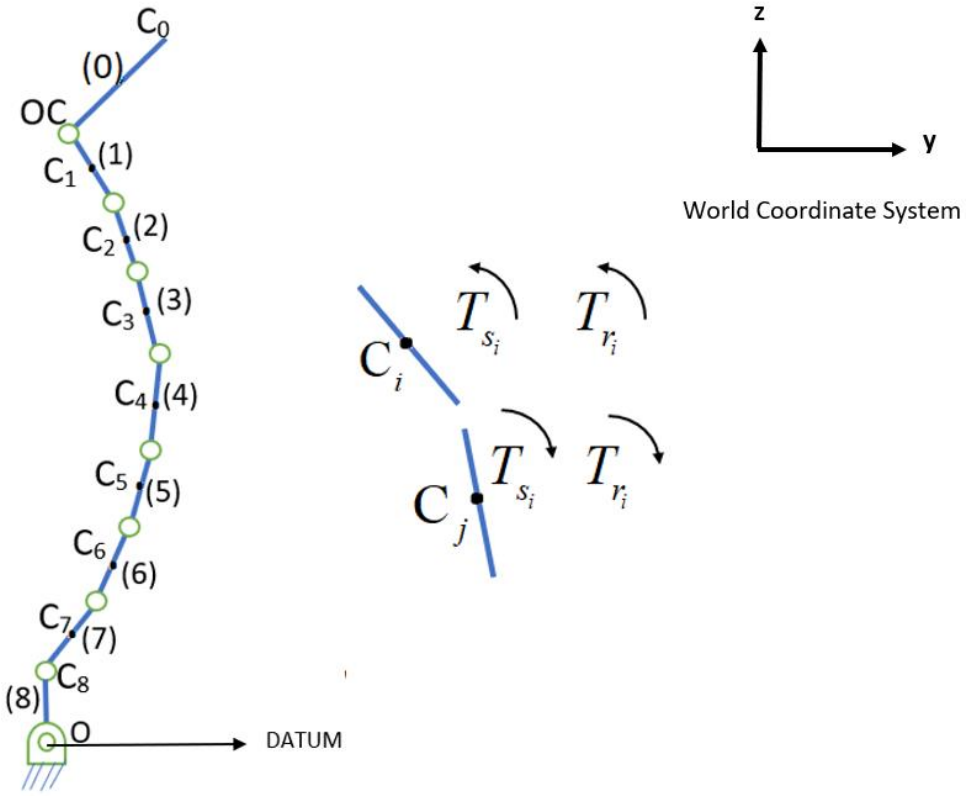

Figure 36. Head Neck spine schematic view with resistive torques and static torques on adjacent body i and body j

C_i : *center of mass of body i*

b_j : *height of neck segment j*

C_8 : *center of mass of T1*

OC : *occipital condyle*

$\left|\overrightarrow{OC\,C_0}\right| = r_0$

T_{s_i} : *static torque applied on body i*

T_{r_i} : *resistive torque applied on body i*

(torsional springs)

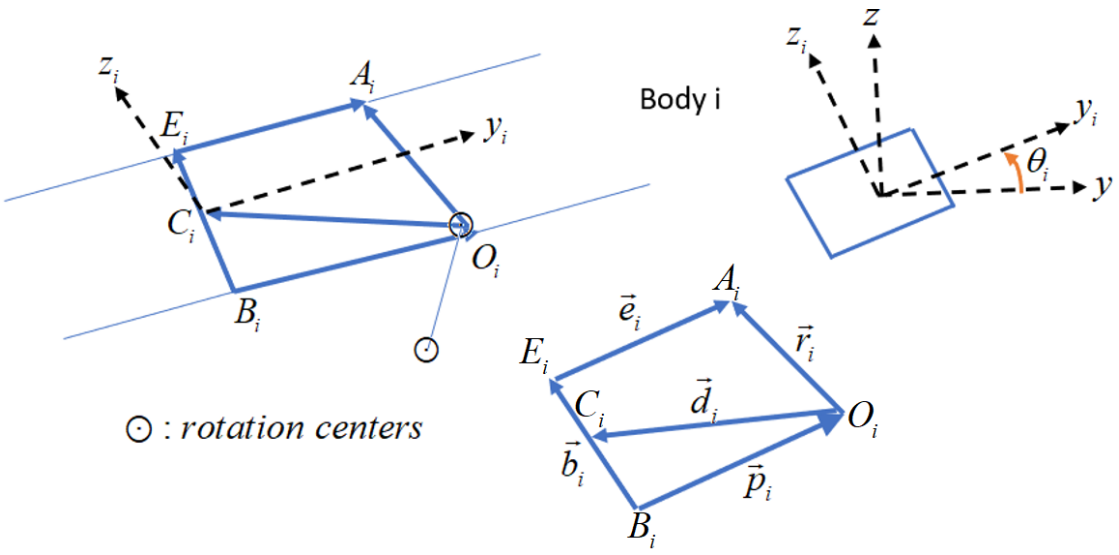

Figure 37. Inertial frame, body frame (on up right corner) and vector expressions on body i between rotation centers

r_i : vector joining rotation centers on body i $\overrightarrow{O_iA_i} = \vec{r}_i$

$\overrightarrow{B_iO_i} = \vec{p}_i$, $\overrightarrow{E_iA_i} = \vec{e}_i$, $\overrightarrow{B_iE_i} = \vec{b}_i$, $\overrightarrow{O_iC_i} = \vec{d}_i$

Position of C_i *with respect to* O *is* $\overrightarrow{OC_i} = \overrightarrow{OO_i} + \overrightarrow{O_iC_i}$

$\vec{p}_i + \vec{d}_i = \vec{b}_i / 2 \Rightarrow \overrightarrow{O_iC_i} = \vec{d}_i = \vec{b}_i / 2 - \vec{p}_i$ *where* $\vec{p}_i = p_i\vec{u}_2^{(i)}$ *and* $\vec{b}_i = b_i\vec{u}_3^{(i)}$

$\vec{e}_i = e_i\vec{u}_2^{(i)}$ $\vec{d}_i = d_{i2}\vec{u}_2^{(i)} + d_{i3}\vec{u}_3^{(i)}$, *we have also* $\vec{p}_i + \vec{r}_i = \vec{b}_i + \vec{e}_i \Rightarrow$

$\vec{r}_i = \vec{b}_i + \vec{e}_i - \vec{p}_i = \vec{r}_{i2}\vec{u}_2^{(i)} + \vec{r}_{i3}\vec{u}_3^{(i)}$,

$\vec{d}_i = (b_i / 2)\vec{u}_3^{(i)} - \vec{p}_i\vec{u}_2^{(i)} \Rightarrow \bar{d}_i^{(i)} = -p_i\bar{u}_2 + (b_i / 2)\bar{u}_3 = d_{i2}\bar{u}_2 + d_{i3}\bar{u}_3$

$\vec{r}_i = b_i\vec{u}_3^{(i)} + e_i\vec{u}_2^{(i)} - \vec{p}_i\vec{u}_2^{(i)} \Rightarrow \bar{r}_i^{(i)} = (e_i - p_i)\bar{u}_2 + b_i\bar{u}_3 = r_{i2}\bar{u}_2 + r_{i3}\bar{u}_3$

$\overrightarrow{OC_i} = \overrightarrow{OO_i} + \overrightarrow{O_iC_i} = \overrightarrow{OO_i} + \vec{d}_i$ expressing in world coordinate system

$\overline{OC_i}^{(w)} = \overline{OO_i}^{(w)} + \bar{d}_i^{(w)}$

$\bar{d}_i^{(w)} = \hat{C}^{(w,i)}\bar{d}_i^{(i)} = e^{\tilde{u}_1\theta_i}(d_{i2}\bar{u}_2 + d_{i3}\bar{u}_3) = d_{i2}(\bar{u}_2\cos\theta_i + \bar{u}_3\sin\theta_i) + d_{i3}(\bar{u}_3\cos\theta_i - \bar{u}_2\sin\theta_i)$

$\bar{d}_i^{(w)} = \bar{u}_2(d_{i2}\cos\theta_i - d_{i3}\sin\theta_i) + \bar{u}_3(d_{i2}\sin\theta_i + d_{i3}\cos\theta_i)$

$\bar{r}_i^{(w)} = \hat{C}^{(w,i)}\bar{r}_i^{(i)} = e^{\tilde{u}_1\theta_i}\bar{r}_i^{(i)} = \bar{u}_2(r_{i2}\cos\theta_i - r_{i3}\sin\theta_i) + \bar{u}_3(r_{i2}\sin\theta_i + r_{i3}\cos\theta_i)$

Body 8: $\overrightarrow{OC_8} = (b_8 / 2)\vec{u}_3^{(8)}$, $\overline{OC_8}^{(w)} = e^{\tilde{u}_1\theta_8}(b_8 / 2)\bar{u}_3 = (b_8 / 2)(\bar{u}_3\cos\theta_8 - \bar{u}_2\sin\theta_8) = \bar{r}_8^{(w)}$

U_i : *Potential energy of body* i $(i = 0,1,2...8)$

$U_8 = m_8 g(b_8 / 2)\cos\theta_8$

$$Body\,7:\overrightarrow{OC_7}=\overrightarrow{OO_7}+\overrightarrow{O_7C_7}=\overrightarrow{OC_8}+\vec{d}_7\Rightarrow\overrightarrow{OC_7}^{(w)}=\overrightarrow{OC_8}^{(w)}+\bar{d}_7^{(w)}$$

$$U_7=m_7g[(\mathrm{b}_8/2)\cos\theta_8+(d_{72}\sin\theta_7+d_{73}\cos\theta_7)]$$

$$Body\,6:\overrightarrow{OC_6}=\overrightarrow{OO_6}+\overrightarrow{O_6C_6}=\vec{r}_8+\vec{r}_7+\vec{d}_6$$

$$U_6=m_6g[(\mathrm{b}_8/2)\cos\theta_8+(\mathrm{r}_{72}\sin\theta_7+r_{73}\cos\theta_7)+(d_{62}\sin\theta_6+d_{63}\cos\theta_6)]$$

$$Body\,5:\overrightarrow{OC_5}=\overrightarrow{OO_5}+\overrightarrow{O_5C_5}=\vec{r}_8+\vec{r}_7+\vec{r}_6+\vec{d}_5$$

$$U_5=m_5g[(\mathrm{b}_8/2)\cos\theta_8+(\mathrm{r}_{72}\sin\theta_7+r_{73}\cos\theta_7)+(\mathrm{r}_{62}\sin\theta_6+r_{63}\cos\theta_6)$$
$$+(d_{52}\sin\theta_5+d_{53}\cos\theta_5)]$$

$$Body\,4:\overrightarrow{OC_4}=\overrightarrow{OO_4}+\overrightarrow{O_4C_4}=\vec{r}_8+\vec{r}_7+\vec{r}_6+\vec{r}_5+\vec{d}_4$$

$$U_4=m_4g[(\mathrm{b}_8/2)\cos\theta_8+(\mathrm{r}_{72}\sin\theta_7+r_{73}\cos\theta_7)+(\mathrm{r}_{62}\sin\theta_6+r_{63}\cos\theta_6)+$$
$$(\mathrm{r}_{52}\sin\theta_5+r_{53}\cos\theta_5)+(d_{42}\sin\theta_4+d_{43}\cos\theta_4)]$$

$$Body\,3:\overrightarrow{OC_3}=\overrightarrow{OO_3}+\overrightarrow{O_3C_3}=\vec{r}_8+\vec{r}_7+\vec{r}_6+\vec{r}_5+\vec{r}_4+\vec{d}_3$$

$$U_3=m_3g[(\mathrm{b}_8/2)\cos\theta_8+(\mathrm{r}_{72}\sin\theta_7+r_{73}\cos\theta_7)+(\mathrm{r}_{62}\sin\theta_6+r_{63}\cos\theta_6)+$$
$$(\mathrm{r}_{52}\sin\theta_5+r_{53}\cos\theta_5)+(\mathrm{r}_{42}\sin\theta_4+r_{43}\cos\theta_4)+(d_{32}\sin\theta_3+d_{33}\cos\theta_3)]$$

$$Body\,2:\overrightarrow{OC_2}=\overrightarrow{OO_2}+\overrightarrow{O_2C_2}=\vec{r}_8+\vec{r}_7+\vec{r}_6+\vec{r}_5+\vec{r}_4+\vec{r}_3+\vec{d}_2$$

$$U_2=m_2g[(\mathrm{b}_8/2)\cos\theta_8+(\mathrm{r}_{72}\sin\theta_7+r_{73}\cos\theta_7)+(\mathrm{r}_{62}\sin\theta_6+r_{63}\cos\theta_6)+$$
$$(\mathrm{r}_{52}\sin\theta_5+r_{53}\cos\theta_5)+(\mathrm{r}_{42}\sin\theta_4+r_{43}\cos\theta_4)+(\mathrm{r}_{32}\sin\theta_3+r_{33}\cos\theta_3)+$$
$$(d_{22}\sin\theta_2+d_{23}\cos\theta_2)]$$

$$Body\ 1:\ \overrightarrow{OC_1} = \overrightarrow{OO_1} + \overrightarrow{O_1C_1} = \vec{r}_8 + \vec{r}_7 + \vec{r}_6 + \vec{r}_5 + \vec{r}_4 + \vec{r}_3 + \vec{r}_2 + \vec{d}_1$$

$$U_1 = m_1 g[(\mathrm{b}_8/2)\cos\theta_8 + (\mathrm{r}_{72}\sin\theta_7 + r_{73}\cos\theta_7) + (\mathrm{r}_{62}\sin\theta_6 + r_{63}\cos\theta_6) + (\mathrm{r}_{52}\sin\theta_5 + r_{53}\cos\theta_5) + (\mathrm{r}_{42}\sin\theta_4 + r_{43}\cos\theta_4) + (\mathrm{r}_{32}\sin\theta_3 + r_{33}\cos\theta_3) + (\mathrm{r}_{22}\sin\theta_2 + r_{23}\cos\theta_2) + (d_{12}\sin\theta_1 + d_{13}\cos\theta_1)]$$

$$\text{Body } 0:\ \overrightarrow{OC_0} = \vec{r}_8 + \vec{r}_7 + \vec{r}_6 + \vec{r}_5 + \vec{r}_4 + \vec{r}_3 + \vec{r}_2 + \vec{r}_1 + \vec{r}_0 = \sum_{k=0}^{8} \vec{r}_k$$

$$U_0 = m_0 g[(\mathrm{b}_8/2)\cos\theta_8 + (\mathrm{r}_{72}\sin\theta_7 + r_{73}\cos\theta_7) + (\mathrm{r}_{62}\sin\theta_6 + r_{63}\cos\theta_6) + (\mathrm{r}_{52}\sin\theta_5 + r_{53}\cos\theta_5) + (\mathrm{r}_{42}\sin\theta_4 + r_{43}\cos\theta_4) + (\mathrm{r}_{32}\sin\theta_3 + r_{33}\cos\theta_3) + (\mathrm{r}_{22}\sin\theta_2 + r_{23}\cos\theta_2) + (\mathrm{r}_{12}\sin\theta_1 + r_{13}\cos\theta_1) + r_0\sin\theta_0]$$

$$Total\ \ potential\ energy\ of\ bodies:\ U = \sum_{k=0}^{8} U_i,$$

$$\frac{\partial U}{\partial \theta_0} = m_0 g r_0 \cos\theta_0 = U_{d_0}$$

$$\frac{\partial U}{\partial \theta_1} = m_0 g(r_{12}\cos\theta_1 - r_{13}\sin\theta_1) + m_1 g(\mathrm{d}_{12}\cos\theta_1 - \mathrm{d}_{13}\sin\theta_1) = U_{d_1}$$

$$\frac{\partial U}{\partial \theta_2} = g(m_0 + m_1)(r_{22}\cos\theta_2 - r_{23}\sin\theta_2) + m_2 g(\mathrm{d}_{22}\cos\theta_2 - \mathrm{d}_{23}\sin\theta_2) = U_{d_2}$$

$$\frac{\partial U}{\partial \theta_3} = g(m_0 + m_1 + \mathrm{m}_2)(r_{32}\cos\theta_3 - r_{33}\sin\theta_3) + m_3 g(\mathrm{d}_{32}\cos\theta_3 - \mathrm{d}_{33}\sin\theta_3) = U_{d_3}$$

$$\frac{\partial U}{\partial \theta_4} = g(m_0 + m_1 + \mathrm{m}_2 + \mathrm{m}_3)(r_{42}\cos\theta_4 - r_{43}\sin\theta_4) +$$
$$m_4 g(\mathrm{d}_{42}\cos\theta_4 - \mathrm{d}_{43}\sin\theta_4) = U_{d_4}$$

$$\frac{\partial U}{\partial \theta_5} = g(m_0 + m_1 + \mathrm{m}_2 + \mathrm{m}_3 + \mathrm{m}_4)(r_{52}\cos\theta_5 - r_{53}\sin\theta_5) +$$
$$m_5 g(\mathrm{d}_{52}\cos\theta_5 - \mathrm{d}_{53}\sin\theta_5) = U_{d_5}$$

$$\frac{\partial U}{\partial \theta_6} = g(m_0 + m_1 + \mathrm{m}_2 + \mathrm{m}_3 + \mathrm{m}_4 + \mathrm{m}_5)(r_{62}\cos\theta_6 - r_{63}\sin\theta_6) +$$
$$m_6 g(\mathrm{d}_{62}\cos\theta_6 - \mathrm{d}_{63}\sin\theta_6) = U_{d_6}$$

$$\frac{\partial U}{\partial \theta_7} = g(m_0 + m_1 + \mathrm{m}_2 + \mathrm{m}_3 + \mathrm{m}_4 + \mathrm{m}_5 + \mathrm{m}_6)(r_{72}\cos\theta_7 - r_{73}\sin\theta_7) +$$
$$m_7 g(\mathrm{d}_{72}\cos\theta_7 - \mathrm{d}_{73}\sin\theta_7) = U_{d_7}$$

$$\frac{\partial U}{\partial \theta_8} = g(m_0 + m_1 + \mathrm{m}_2 + \mathrm{m}_3 + \mathrm{m}_4 + \mathrm{m}_5 + \mathrm{m}_6 + m_7 + \mathrm{m}_8)(\mathrm{b}_8/2)(-\sin\theta_8)$$
$$= g(\sum_{k=0}^{8} m_k)(\mathrm{b}_8/2)(-\sin\theta_8) = U_{d_8}$$

$e_1 = 0,$ $\quad \mathrm{p}_1 = 0.00231\ m$
$e_2 = -0.00175\ m,$ $\quad \mathrm{p}_2 = 0.00173\ m$
$e_3 = -0.00144\ m,$ $\quad \mathrm{p}_3 = 0.00142\ m$
$e_4 = -0.00145\ m,$ $\quad \mathrm{p}_4 = 0.00142\ m$
$e_5 = -0.00136\ m,$ $\quad \mathrm{p}_5 = 0.00134\ m$
$e_6 = -0.00135\ m,$ $\quad \mathrm{p}_6 = 0.00133\ m$
$e_7 = -0.00141\ m,$ $\quad \mathrm{p}_7 = 0.00140\ m$

$$Lagrange\ equations\ for\ static\ equilibrium: \frac{\partial U}{\partial q_k} = Q_k$$

U : *Potential Energy* $\quad Q_k$: *External Moments*

Generalized Coordinates

$\bar{q} = [\theta_0, \theta_1, \theta_2, \theta_3, \theta_4, \theta_5, \theta_6, \theta_7, \theta_8] \qquad \delta W$: *total virtual work*

$$\delta W = T_{s8}\delta\theta_8 + (T_{s7} + T_{r7})(\delta\theta_7 - \delta\theta_8) + (T_{s6} + T_{r6})(\delta\theta_6 - \delta\theta_7) +$$
$$(T_{s5} + T_{r5})(\delta\theta_5 - \delta\theta_6) + (T_{s4} + T_{r4})(\delta\theta_4 - \delta\theta_5) + (T_{s3} + T_{r3})(\delta\theta_3 - \delta\theta_4) +$$
$$(T_{s2} + T_{r2})(\delta\theta_2 - \delta\theta_3) + (T_{s1} + T_{r1})(\delta\theta_1 - \delta\theta_2) + (T_{s0} + T_{r0})(\delta\theta_0 - \delta\theta_1)$$

$$\delta W = \sum_{k=0}^{8} Q_k \delta\theta_k$$

$$Q_0 = T_{s0} + T_{r0} = U_{d_0} \quad \rightarrow \quad T_{s0} = U_{d_0} - T_{r0}$$
$$Q_1 = -(T_{s0} + T_{r0}) + (T_{s1} + T_{r1}) = U_{d_1} \quad \rightarrow \quad T_{s1} = U_{d_1} + (T_{s0} + T_{r0}) - T_{r1}$$
$$Q_2 = -(T_{s1} + T_{r1}) + (T_{s2} + T_{r2}) = U_{d_2} \quad \rightarrow \quad T_{s2} = U_{d_2} + (T_{s1} + T_{r1}) - T_{r2}$$
$$Q_3 = -(T_{s2} + T_{r2}) + (T_{s3} + T_{r3}) = U_{d_3} \quad \rightarrow \quad T_{s3} = U_{d_3} + (T_{s2} + T_{r2}) - T_{r3}$$
$$Q_4 = -(T_{s3} + T_{r3}) + (T_{s4} + T_{r4}) = U_{d_4} \quad \rightarrow \quad T_{s4} = U_{d_4} + (T_{s3} + T_{r3}) - T_{r4}$$
$$Q_5 = -(T_{s4} + T_{r4}) + (T_{s5} + T_{r5}) = U_{d_5} \quad \rightarrow \quad T_{s5} = U_{d_5} + (T_{s4} + T_{r4}) - T_{r5}$$
$$Q_6 = -(T_{s5} + T_{r5}) + (T_{s6} + T_{r6}) = U_{d_6} \quad \rightarrow \quad T_{s6} = U_{d_6} + (T_{s5} + T_{r5}) - T_{r6}$$
$$Q_7 = -(T_{s6} + T_{r6}) + (T_{s7} + T_{r7}) = U_{d_7} \quad \rightarrow \quad T_{s7} = U_{d_7} + (T_{s6} + T_{r6}) - T_{r7}$$
$$Q_8 = -(T_{s7} + T_{r7}) + T_{s8} = U_{d_8} \quad \rightarrow \quad T_{s8} = U_{d_8} + (T_{s7} + T_{r7})$$

Masses and geometric properties of segments are as follows:

$m_0 = 4.6\,kg,\ m_1 = 0.22\,kg,\ m_2 = 0.25\,kg,\ m_3 = 0.24\,kg,\ m_4 = 0.23\,kg,$
$m_5 = 0.23\,kg,\ m_6 = 0.24\ kg,\ m_7 = 0.22\,kg,\ m_8 = 1.0235\,kg$

$r_0 = 59.61\ mm,\ b_1 = 17.4\,mm,\ b_2 = 18.23\,mm,$
$b_3 = b_4 = b_5 = b_6 = b_7 = b_1 = 17.4\,mm,\ b_8 = 16.6\ mm$

Neck segments have their centre of masses at their geometric centres

The arc roughly divides the neck parts in half.

Lagrange equations and parameters were defined in Msc Visual Nastran 4D to evaluate virtual motor torques to balance the head and neck model and simulations were performed.

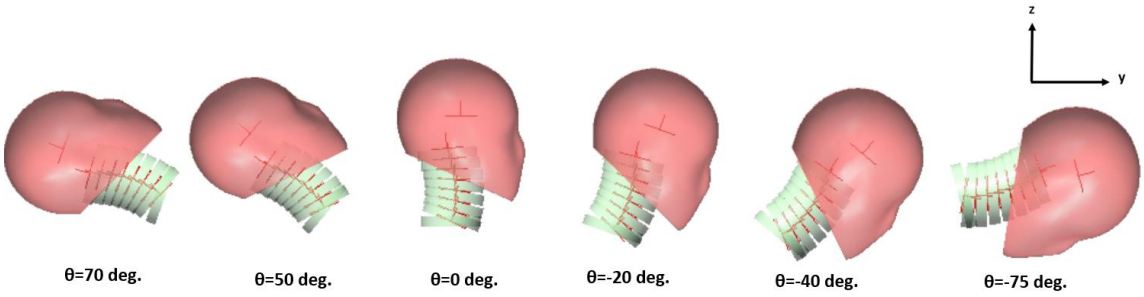

Figure 38. Head and Neck model with muscle tone balanced at different orientations of T1

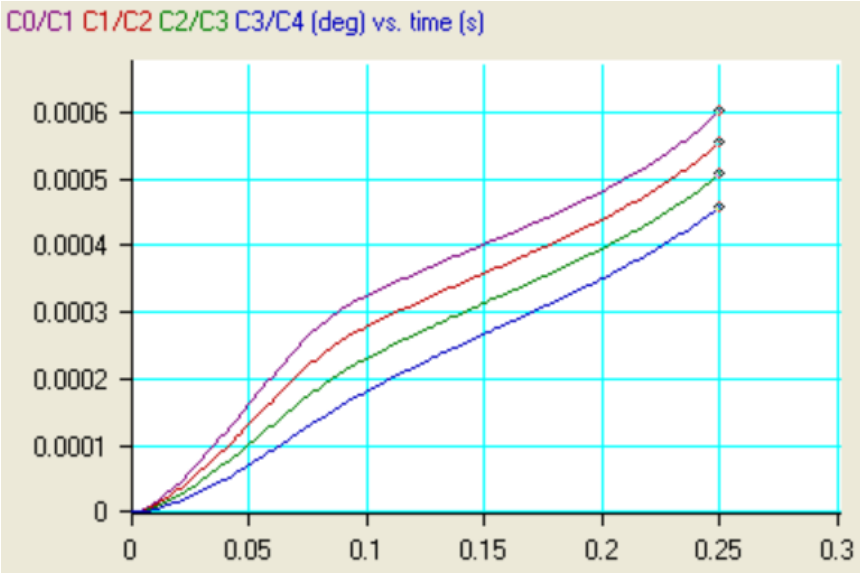

Figure 39. Relative angles(degree) between adjacent bodies (C0-C1, C1-C2, C2-C3,C3-C4) with respect to initial position when simulation run with an orientation of T1 θ=35° and muscle tone integrated into the model

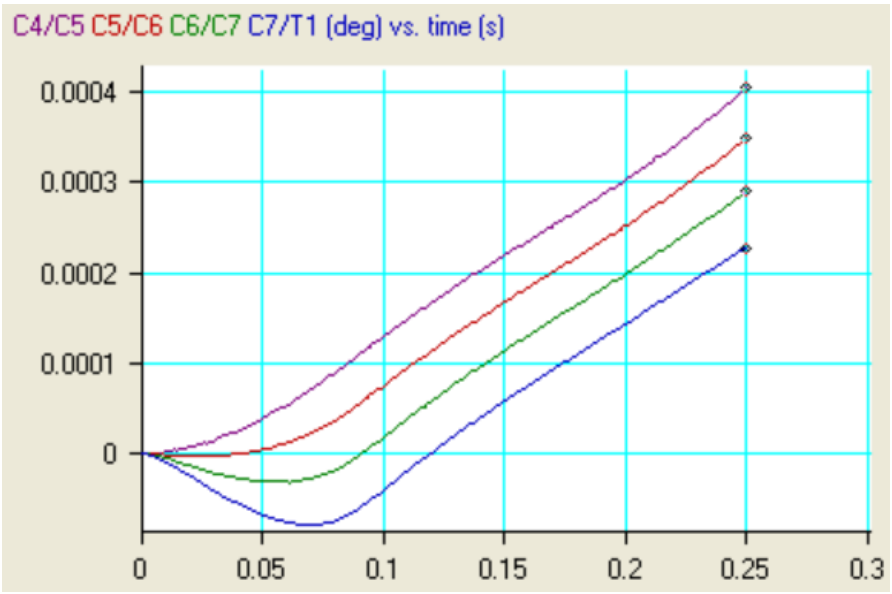

Figure 40. Relative angles(degree) between adjacent bodies (C4-C5, C5-C6,C6-C7,C7-T1) with respect to initial position when simulation run with an orientation of T1 θ=35° and muscle tone integrated into the model

As seen in Fig. 39 and Fig.40 with a 35° orientation of t1 head neck model relative angles between vertebrae are very small amount with a maximum 10^{-4} degree of error which is actually the numerical error software package do solving differential equations. Therefore, the head and neck model is able to maintain its posture.

5.3 Rear Impact Volunteer Tests

An equipment in which the sled is sloped 10 degree from horizontal is seen schematically in Fig. 41. A rigid seat with a seatback angled 20 degrees from vertical was attached to a sled, which was positioned on 4m incline rails slanted 10 degrees from the horizontal line. There was no head rest and safety belt for the rigid seat. By releasing the sled from the top of the rails, the rear-end collision was produced. To slow the sled, a hydraulic damper was installed on the rear rails.[3]

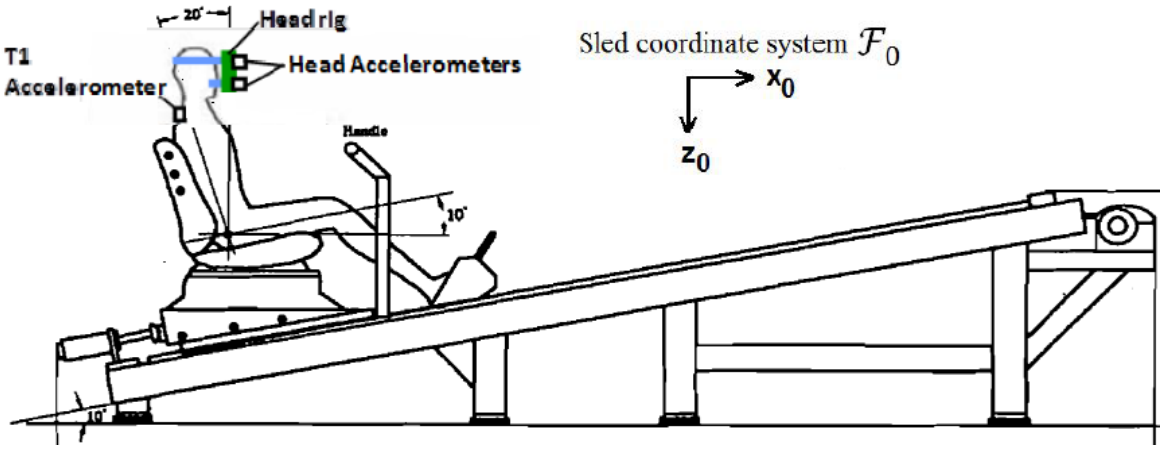

Figure 41. Sled test apparatus for volunteer rear impact. Adapted from([4],[3])

ID	Age(year)	Height(cm)	Weight(kg)
Male 1	22	175	73
Male 2	23	174	71
Male 3	34	176	72
Male 4	25	181	79
Male 5	24	173	65
Male 6	23	178	73
Male 7	33	174	66
Male 8	24	174	71
Male 9	25	176	79
Male 10	22	174	70
Male 11	21	171	69
Male 12	22	172	61

Table 2. Age, Height and Weight details of volunteers in the rear impact tests[3]

12 male volunteers participated in these test series. Their age, height and weight are given in the Table 2. They were asked not to be tense just before the impact. Female volunteers also take part in. However, since the model created embodies 50th percentile male, female responses are out of interest.

To get the head c.g. acceleration, two biaxial accelerometers were installed on the head rig indicated as a green bar in Fig.41. It was connected to the forehead and mouth through a mouthpiece [25]. To measure T1 acceleration, an accelerometer was put on the back surface of T1 vertebra.

Some target markers are mounted to the head and T1 vertebra for video tracking to measure displacements and accelerations of associated bodies.

The sled hit the hydraulic damper with a velocity of 1.722 m/s in negative x direction which resulted in a highest velocity of 0.527 m/s in positive x direction. Peak acceleration of the sled measured 27m/s^2. [25]

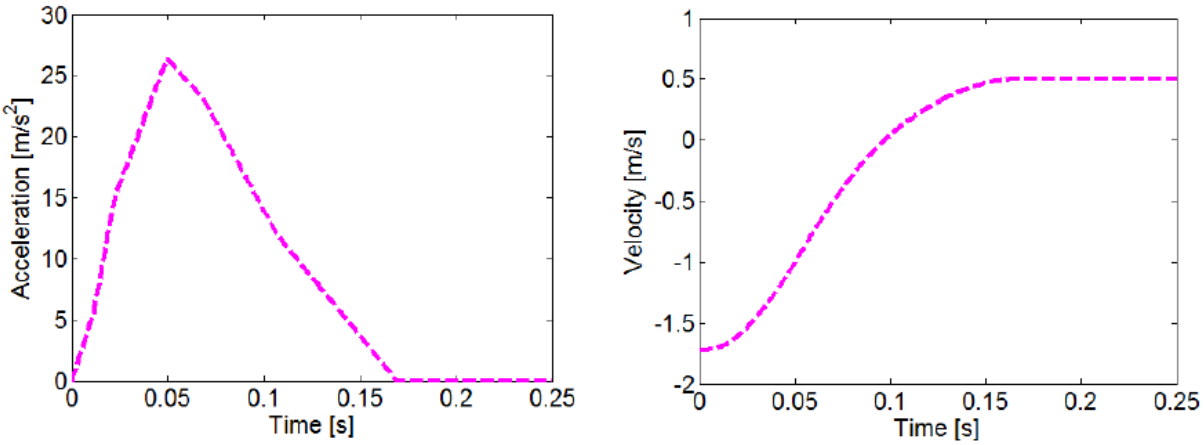

Figure 42. Total Acceleration and velocity of the sled in the rear impact volunteer tests (Taken from [25])

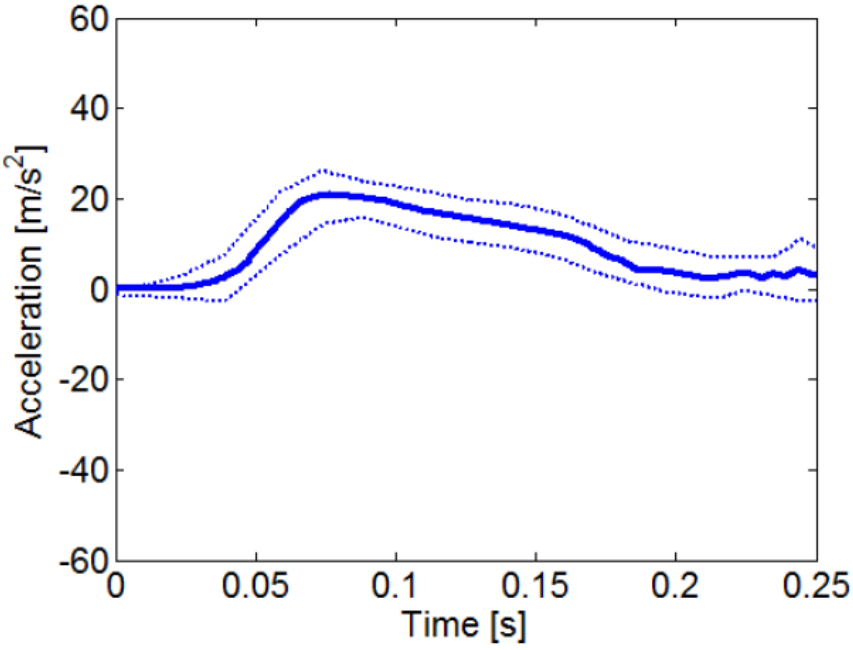

Figure 43. T1 mean x acceleration with one standart deviation in the rear impact volunteer tests [25]

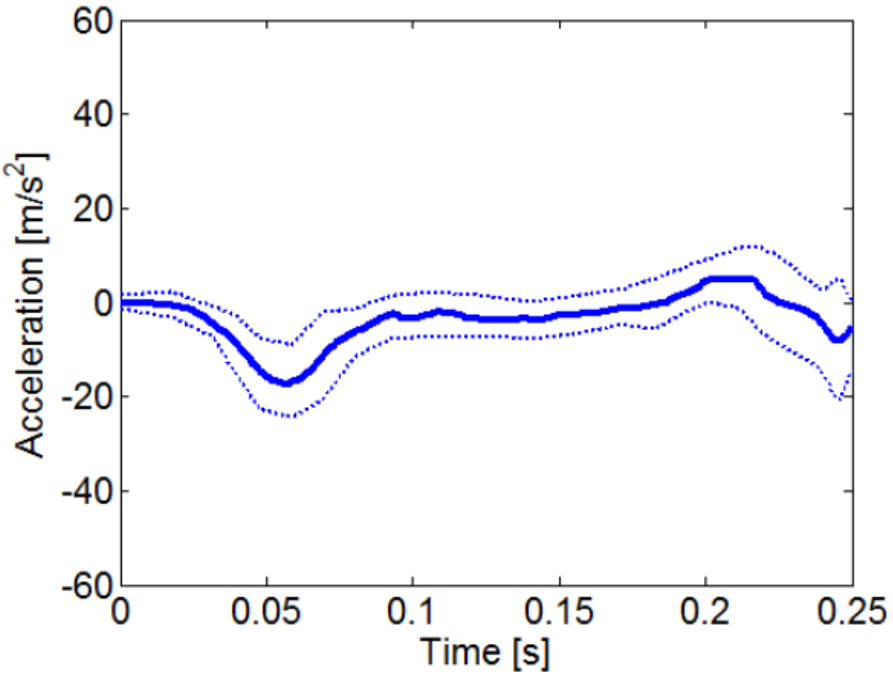

Figure 44. T1 mean z acceleration with one standart deviation in the rear impact volunteer tests [25]

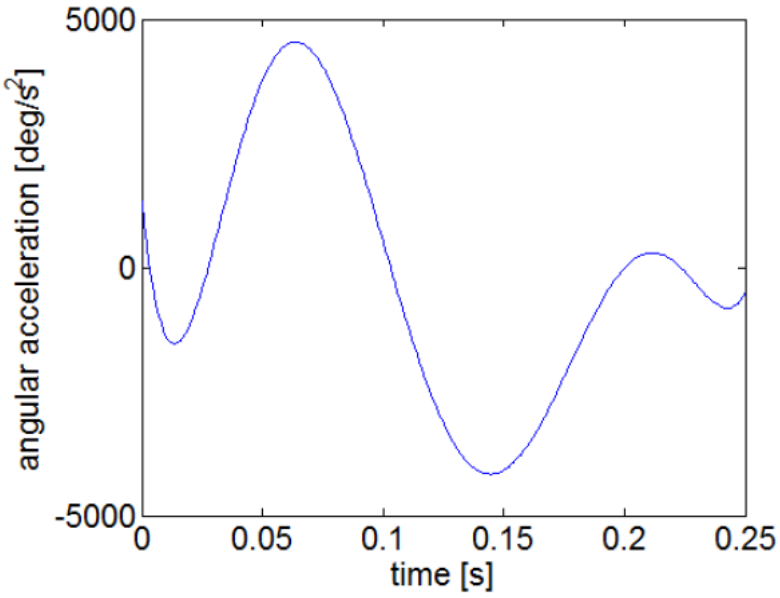

Figure 45. T1 mean angular acceleration in the rear impact volunteer tests [25]

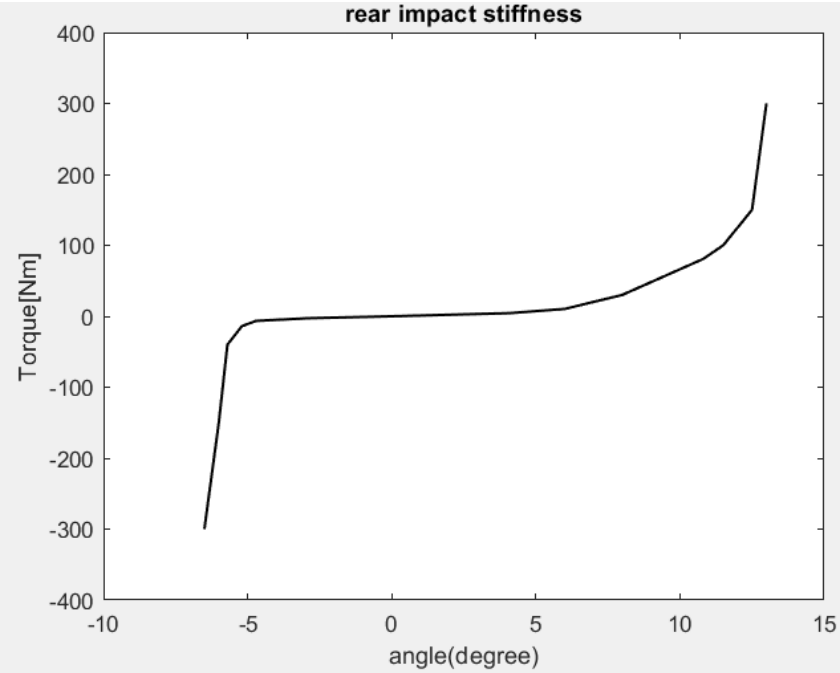

Figure 46. Torques versus angle function used on the model for stiffness values between intervertebral joints for rear impact volunteer data simulation

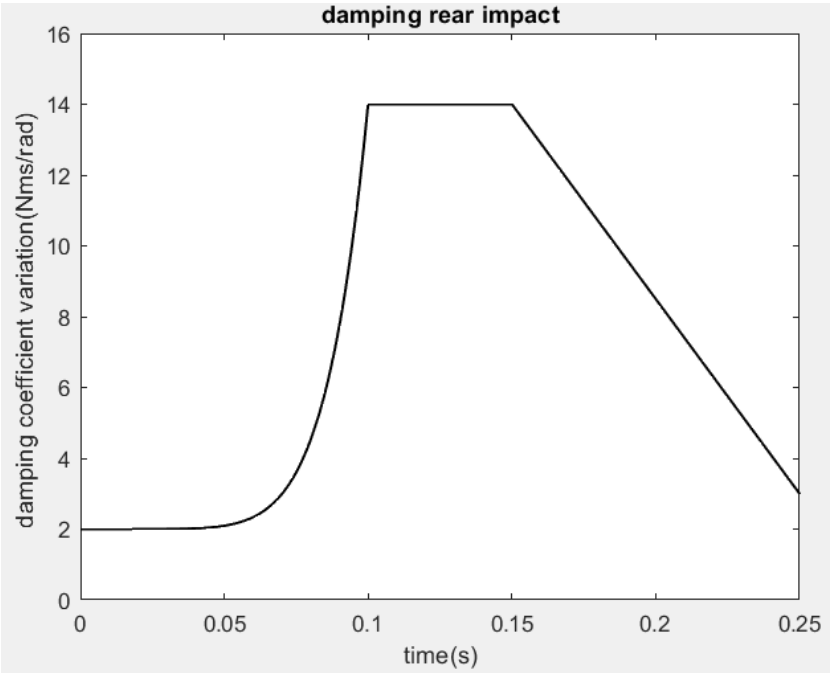

Figure 47. Damping coefficient variation used on the model between intervertebral joints for rear impact volunteer data simulation

5.3.1 Head and Neck Model Responses with Rear Impact Volunteer Test Data

Mean acceleration values indicated on fig.43, fig.44 and fig. 45 for the rear impact volunteer tests are given on the back at T1 as input on the model having muscle tone. Time history of head and neck model is given below with rear impact volunteer test data. Responses are indicated with green dashed line compared with rear impact volunteer corridors from fig.49 through fig.57.

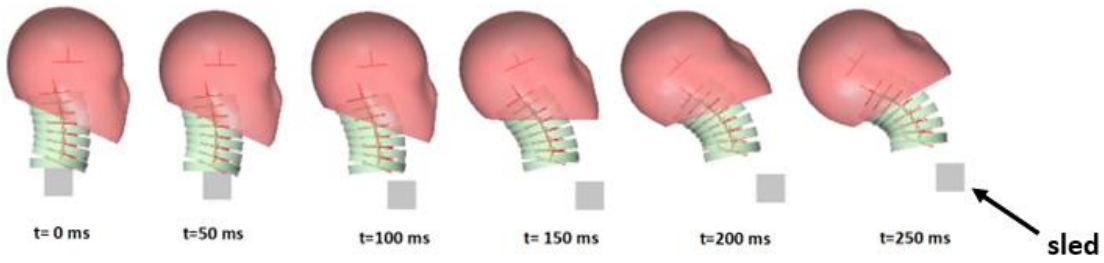

Figure 48. Time history of head neck model simulation with muscle tone using rear impact volunteer test data

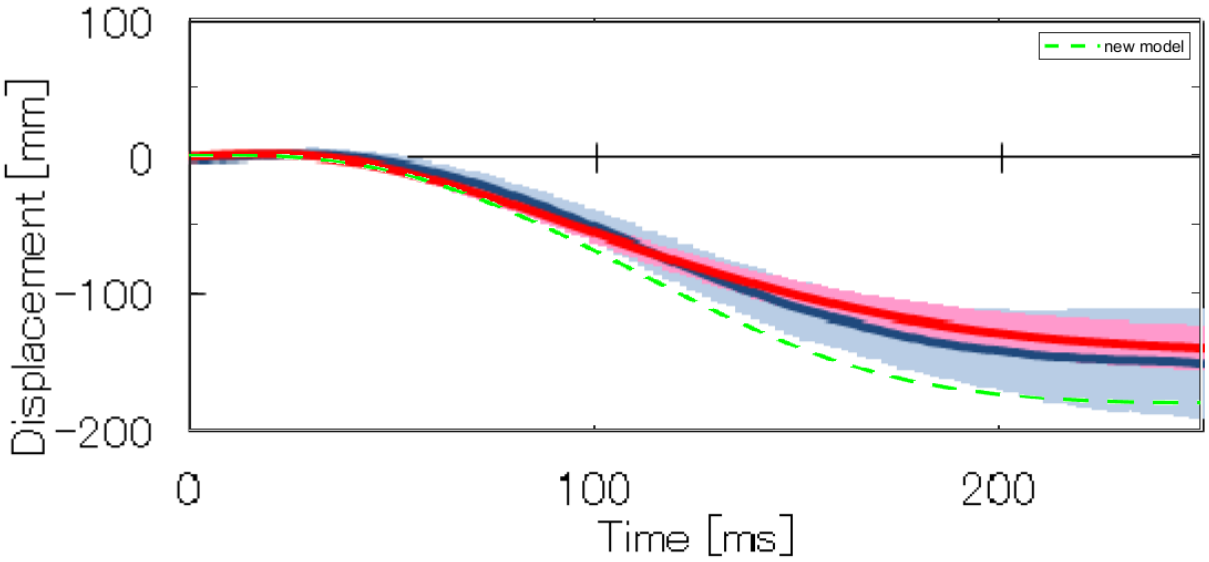

Figure 49. Head CG Displacement relative to sled in X direction expressed in sled coordinate system

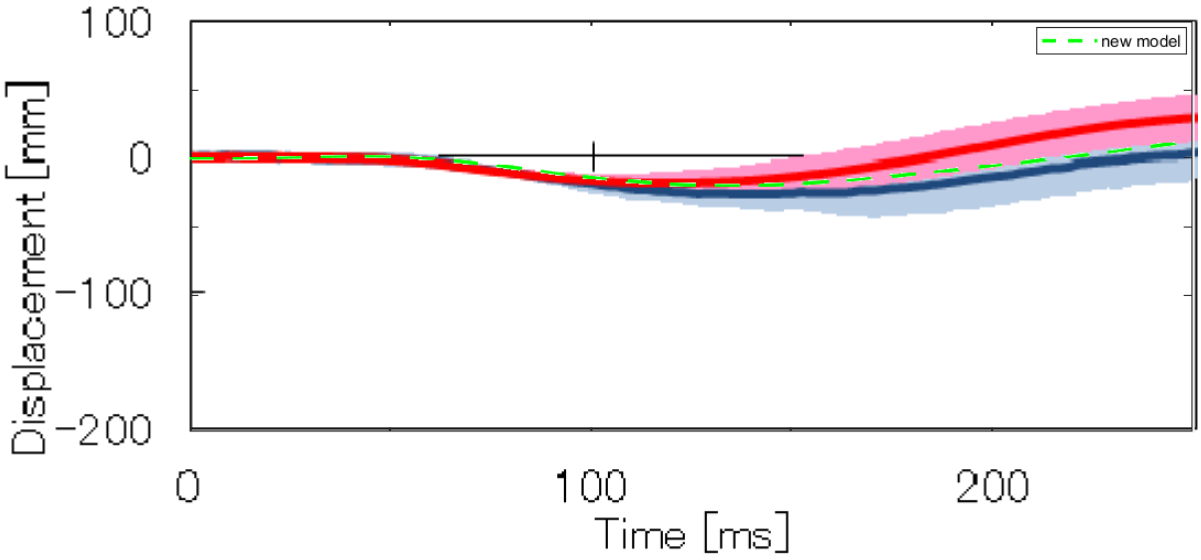

Figure 50. Head CG Displacement relative to sled in Z direction expressed in sled coordinate system

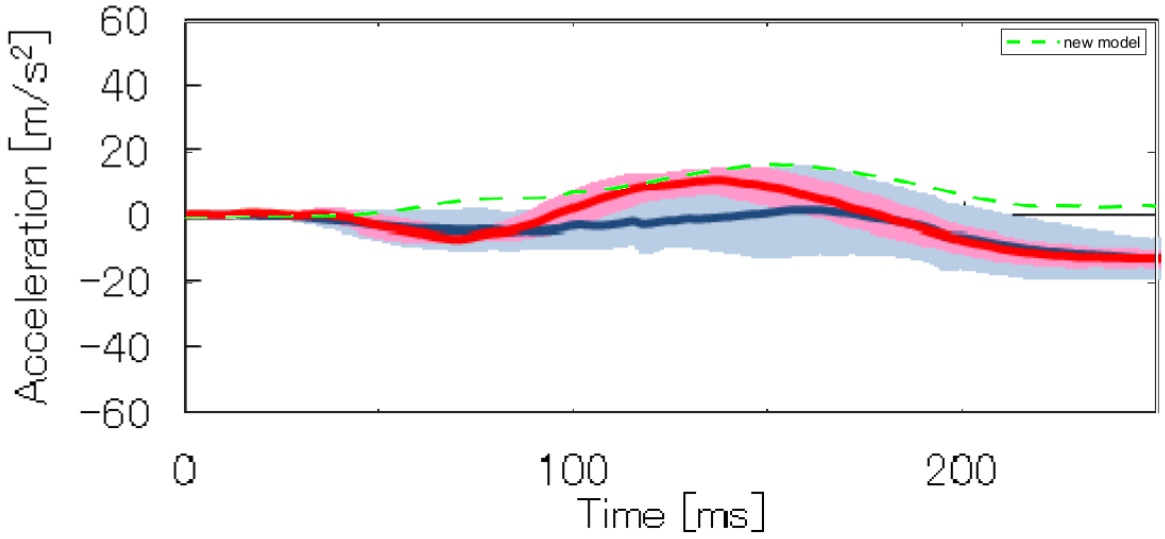

Figure 51. Head CG acceleration in X direction

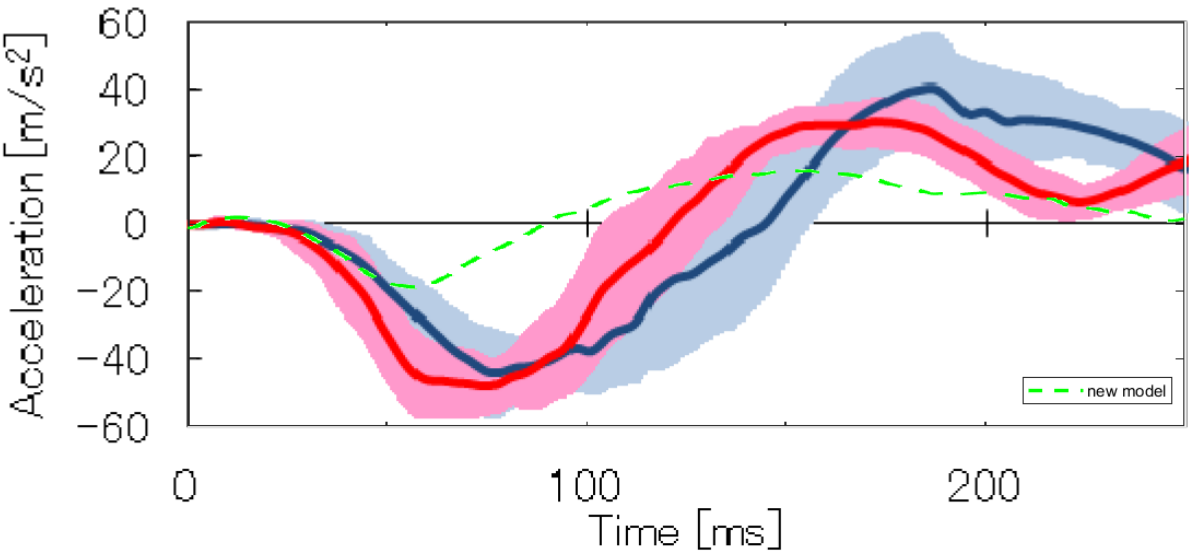

Figure 52. Head CG acceleration in Z direction

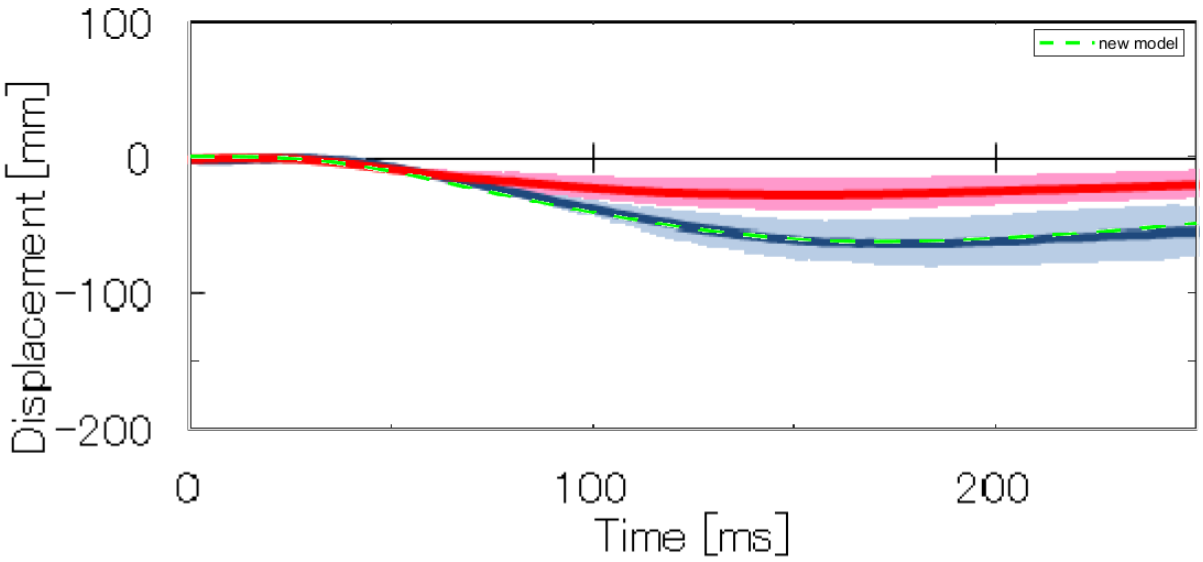

Figure 53. Torso(T1) Displacement relative to sled in X direction expressed in sled coordinate system

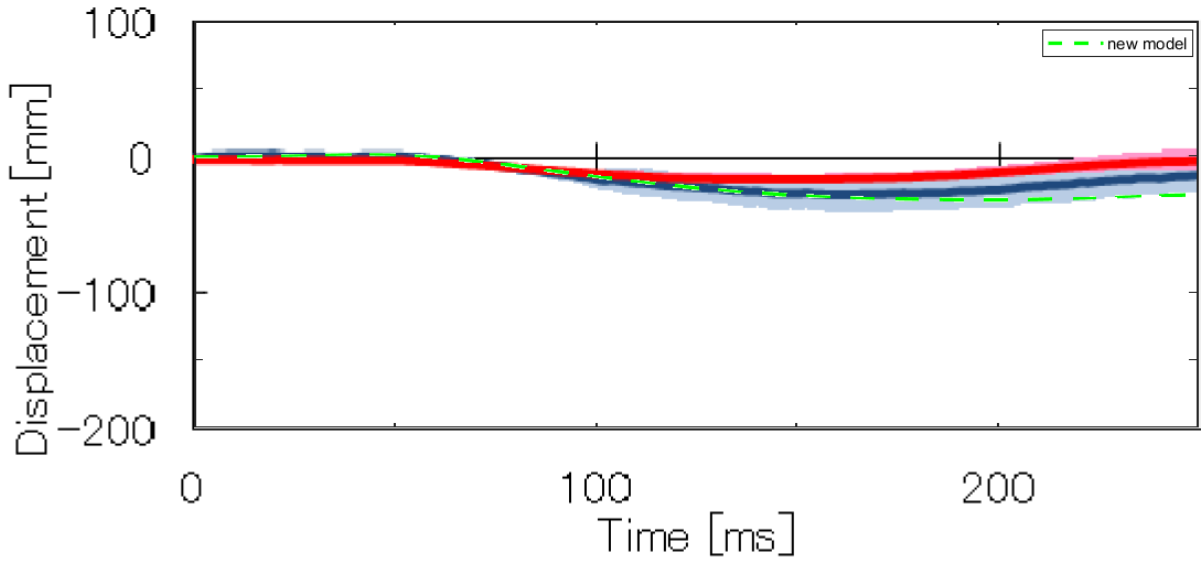

Figure 54. Torso(T1) Displacement relative to sled in Z direction expressed in sled coordinate system

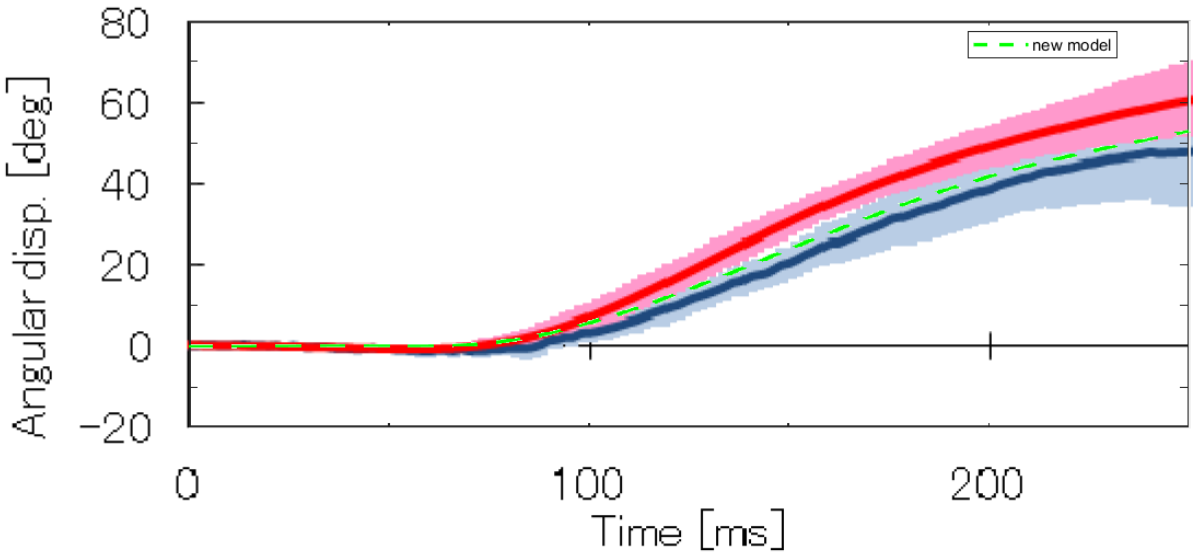

Figure 55. Head rotation relative to sled expressed in sled coordinate system

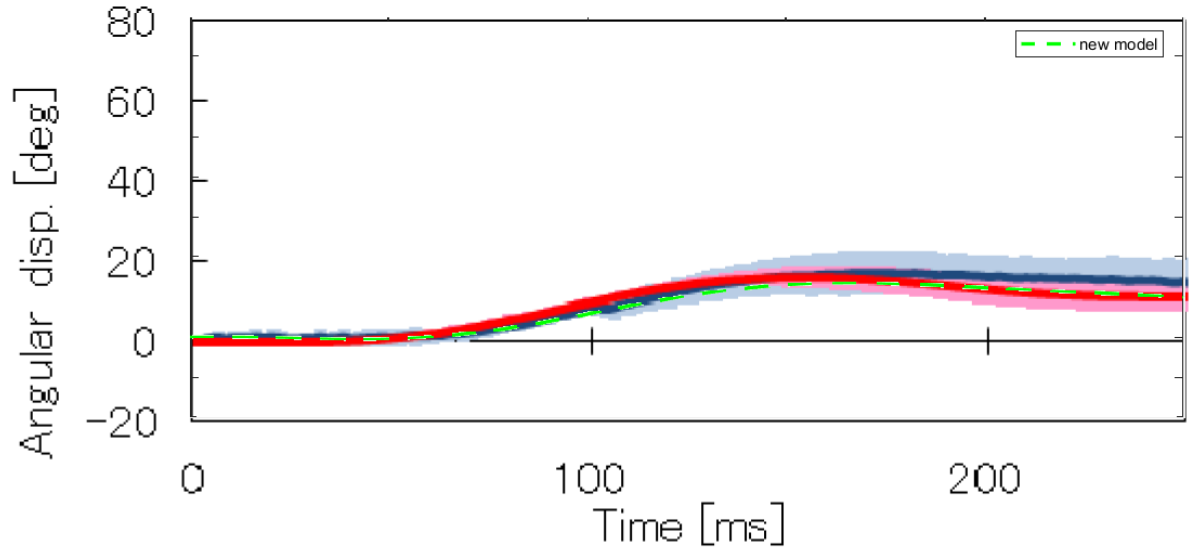

Figure 56. Torso(T1) rotation relative to sled expressed in sled coordinate system

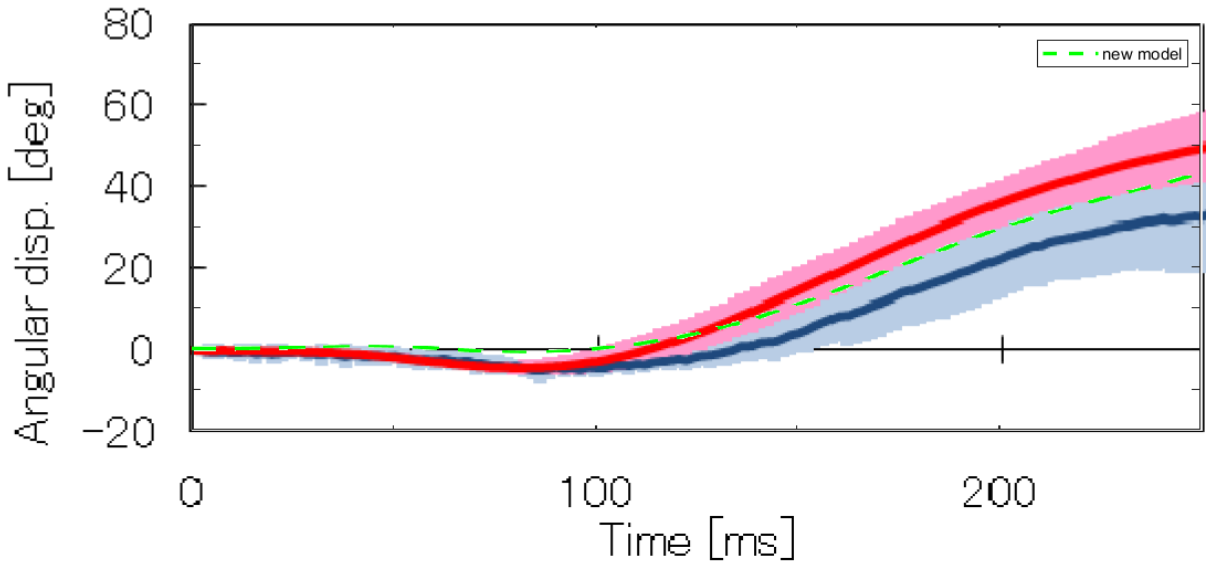

Figure 57. Head rotation with respect to T1(Torso) expressed in Torso Frame

While blue corridors show male volunteer response corridors and dark blue line is average male volunteer response, pink corridors display female response corridors and red line is average female volunteer response.

Responses of the model are in good agreement with male volunteer corridors as one can see.

5.4 Frontal Impact Volunteer Tests

Five volunteers seated on a rigid seat were subjected to a crash pulse with a peak sled acceleration of 15g in the experiments. The seat was attached on a accelerator named HYGE. Average mass, average height of volunteers and peak crash pulse are given on table 3. Not only frontal tests were performed on the volunteers but also lateral impacts with a peak 7g sled acceleration were conducted in Naval Biodynamics Laboratory (NBLD). [1]

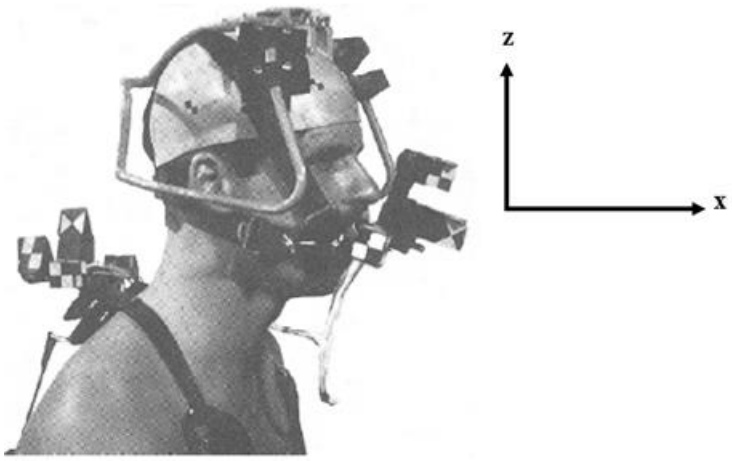

Figure 58. Setup for the frontal impact volunteer tests(taken from[1]) and coordinate system used for head and T1[22]

Parameter	***Value***
Total number of volunteers	5
Total number of tests	9
Average mass	68.6 kg
Average height	1.69 m
Max crash pulse	15 g

Table 3. Frontal impact volunteer test information.[1]

Mean acceleration of T1 in x direction and mean angular acceleration of T1 for the motion are given on the fig 59. And fig.60

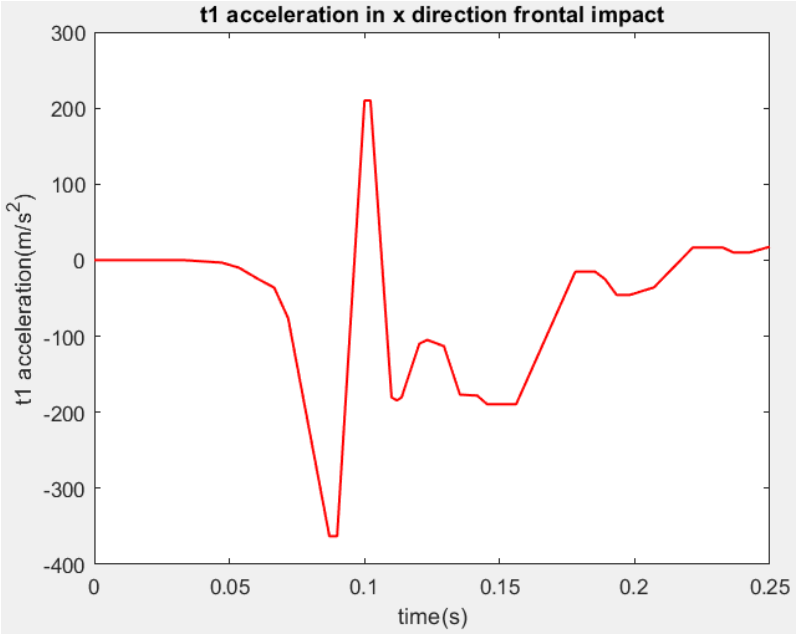

Figure 59. Mean acceleration of T1 in x direction

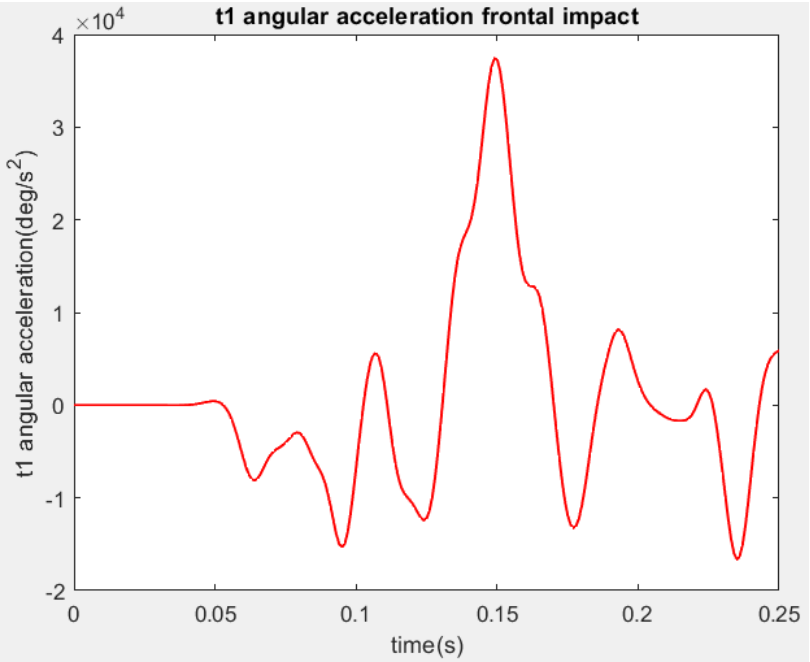

Figure 60. Mean angular acceleration of T1

The mean acceleration of T1 in z direction is negligible in the experiment.[1] Therefore, there is no acceleration input on front at T1 in z direction.

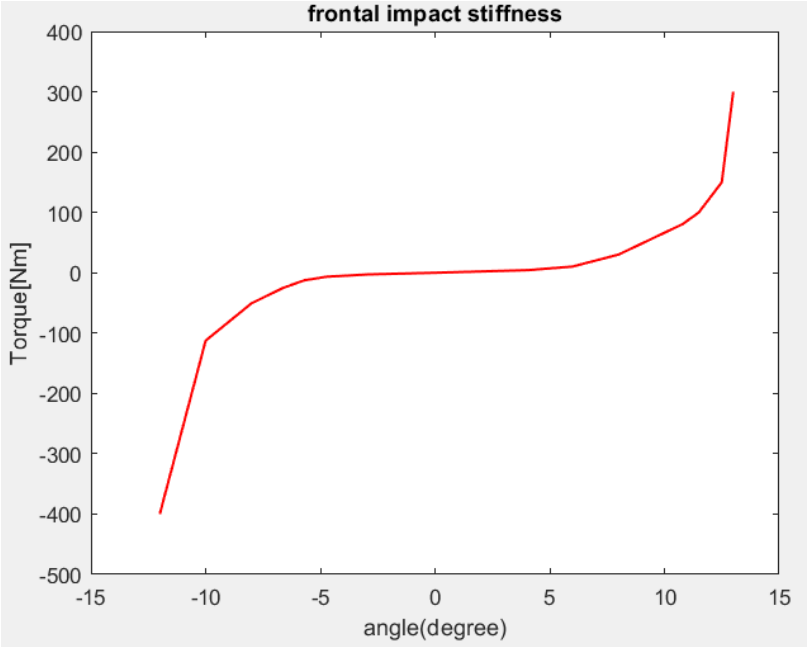

Figure 61. Torques versus angle function used on the model for stiffness values between intervertebral joints for frontal impact volunteer data simulation

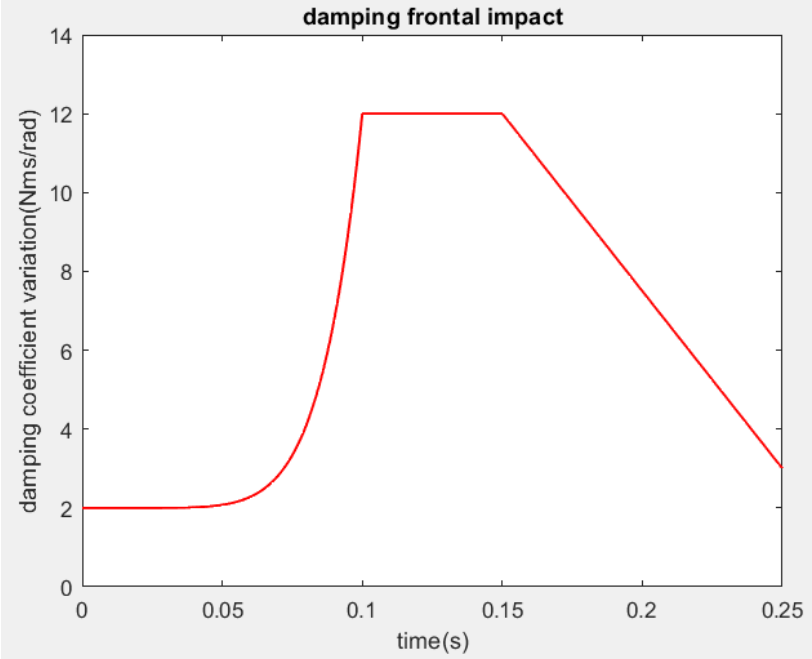

Figure 62. Damping coefficient variation used on the model between intervertebral joints for frontal impact volunteer data simulation

5.4.1 Head and Neck Model Responses with Frontal Impact Volunteer Test Data

T1 Acceleration values of average response on fig.59 and on fig.60 for the volunteers are given as input on the front at T1 on the head and neck model having muscle tone. Results with volunteer corridors are compared with multi-body model of Van der Horst with active muscles and passive muscles seperately included as following.

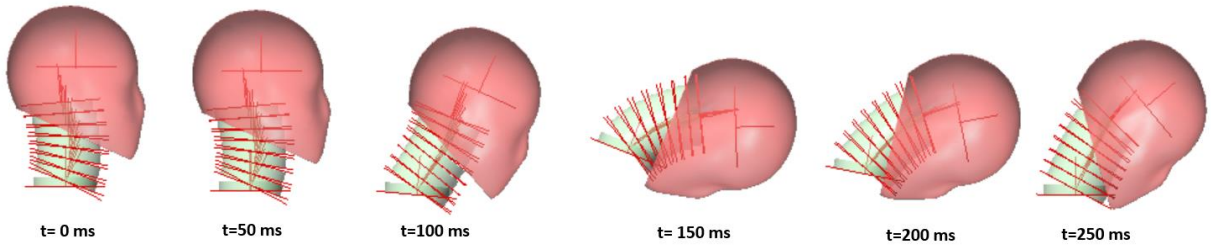

Figure 63. Time history of head and neck model with muscle tone using frontal impact volunteer test data

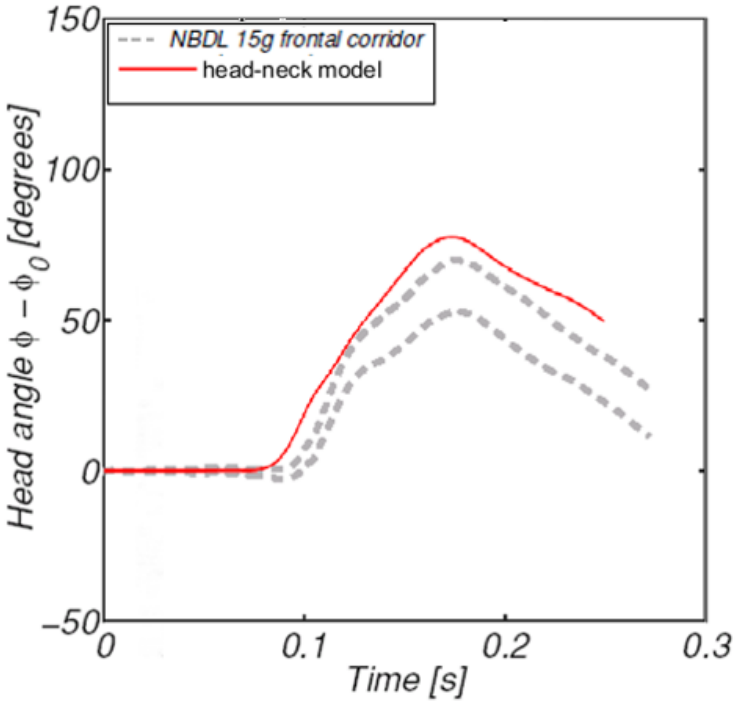

Figure 64. Orientation of head with respect to torso compared with volunteers corridor

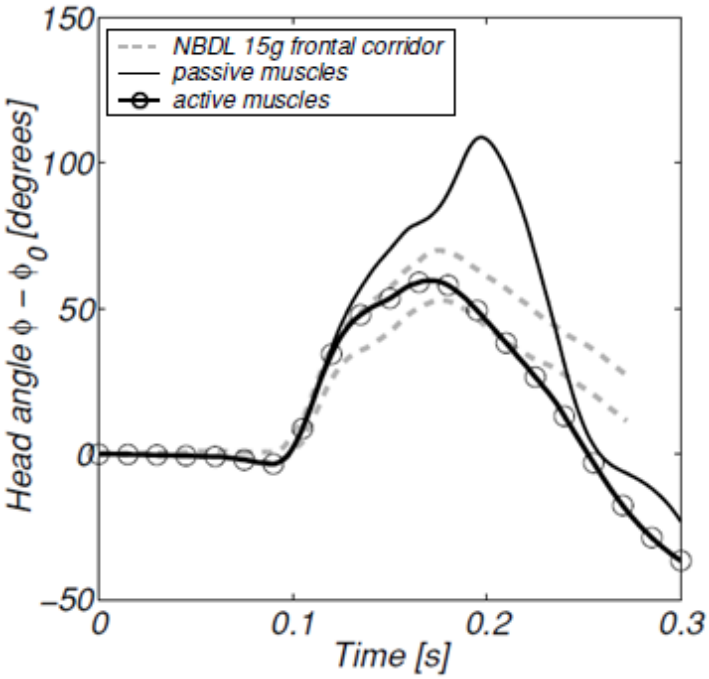

Figure 65. Orientation of head with respect to torso compared with volunteers corridor Model of Van Der Horst (Adapted From [1])

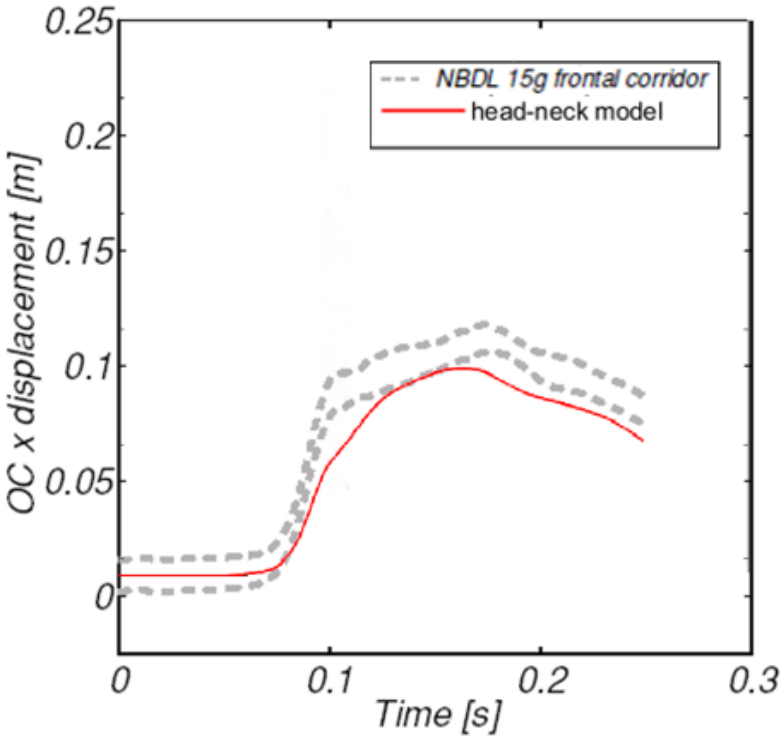

Figure 66. Displacement of Occipital Condyles (OC) with respect to torso in x direction (expressed in torso frame) compared with volunteers corridor

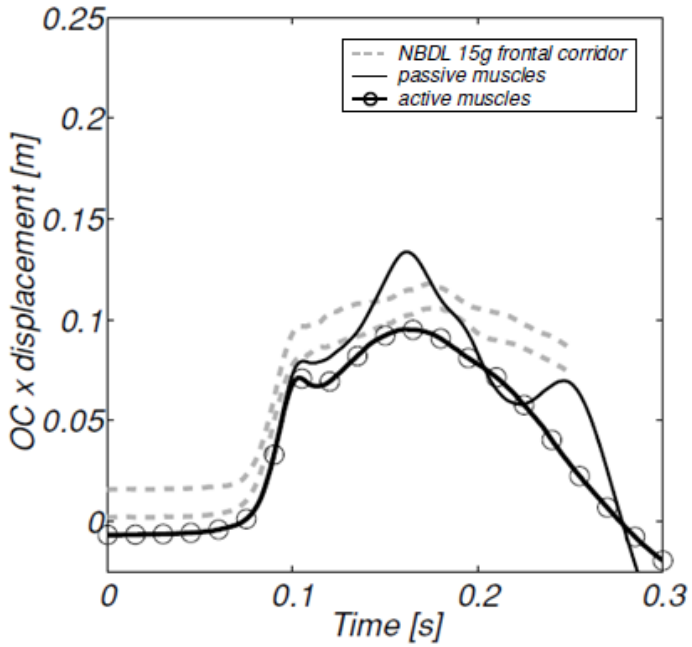

Figure 67. Displacement of Occipital Condyles (OC) with respect to torso in x direction (expressed in torso frame) compared with volunteers corridor Model of Van Der Horst (Adapted From [1])

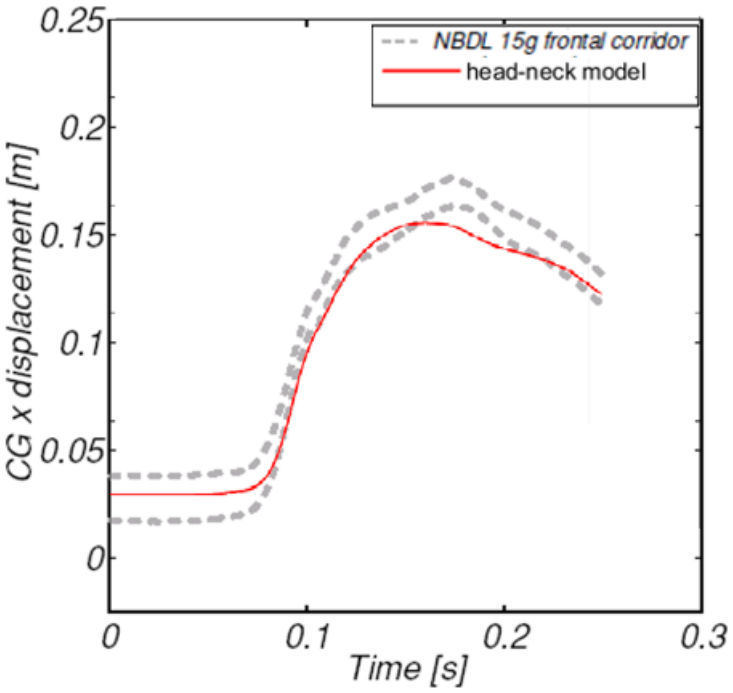

Figure 68. Displacement of Head cg with respect to torso in x direction (expressed in torso frame) compared with volunteers corridor

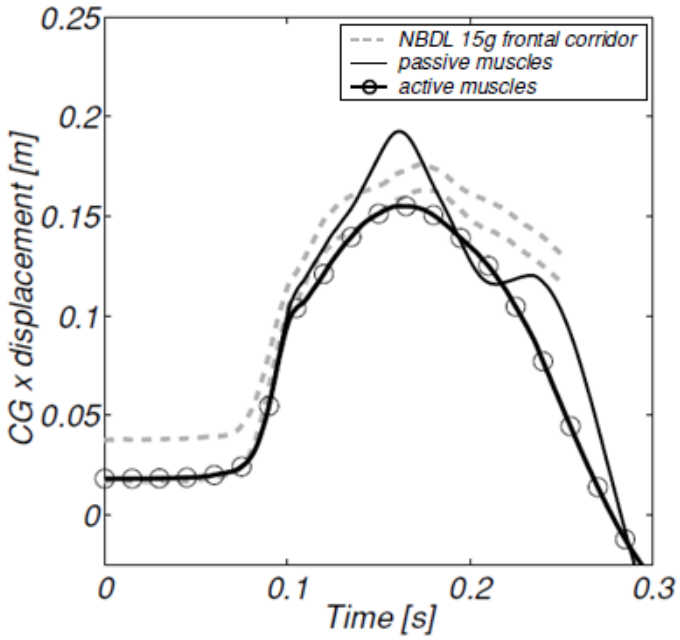

Figure 69. Displacement of Head cg with respect to torso in x direction (expressed in torso frame) compared with volunteers corridor Model of Van Der Horst (Adapted From [1])

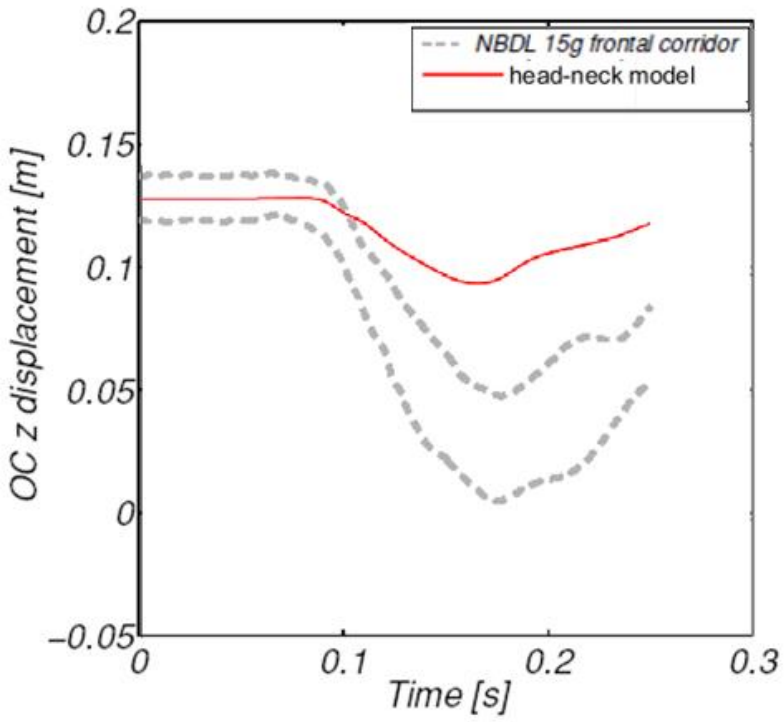

Figure 70. Displacement of Occipital Condyles (OC) with respect to torso in z direction (expressed in torso frame) compared with volunteers corridor

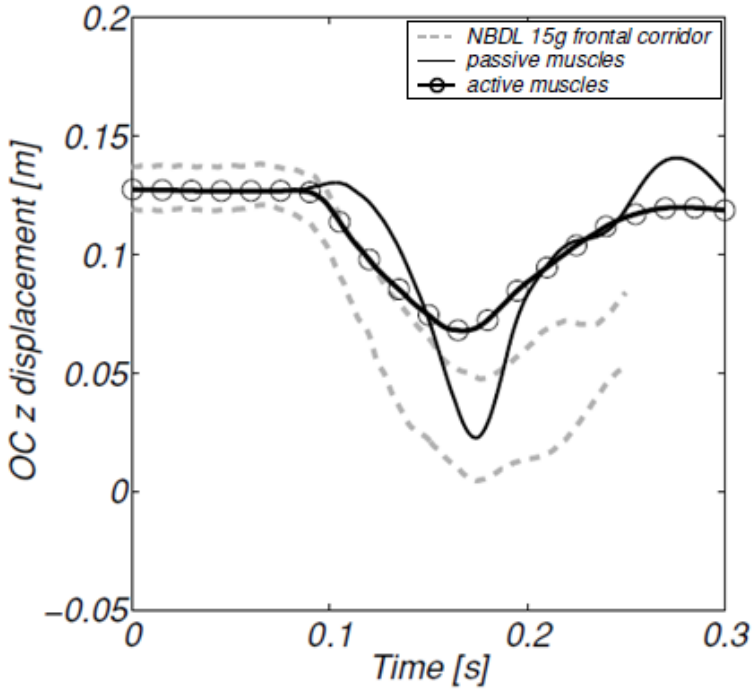

Figure 71. Displacement of Occipital Condyles (OC) with respect to torso in z direction (expressed in torso frame) compared with volunteers corridor Model of Van Der Horst (Adapted From [1])

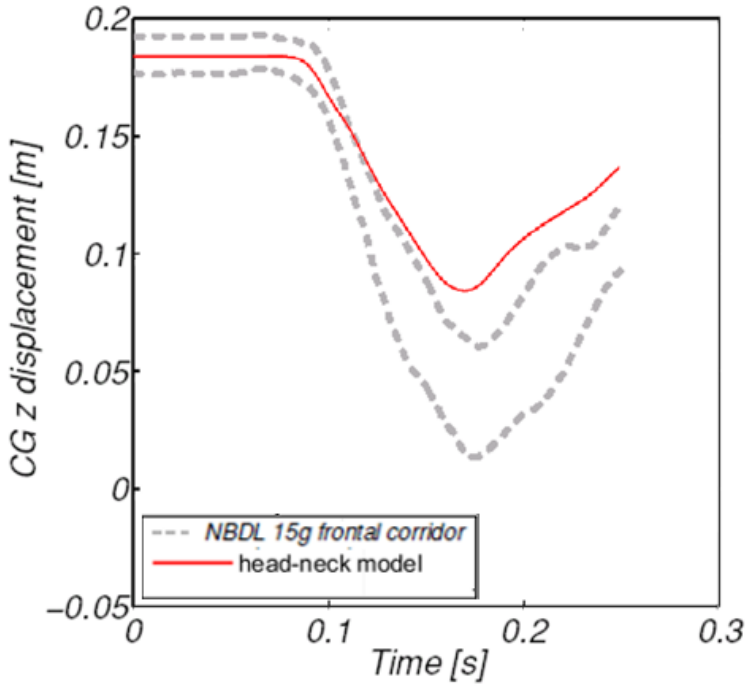

Figure 72. Displacement of Head cg with respect to torso in z direction (expressed in torso frame) compared with volunteers corridor

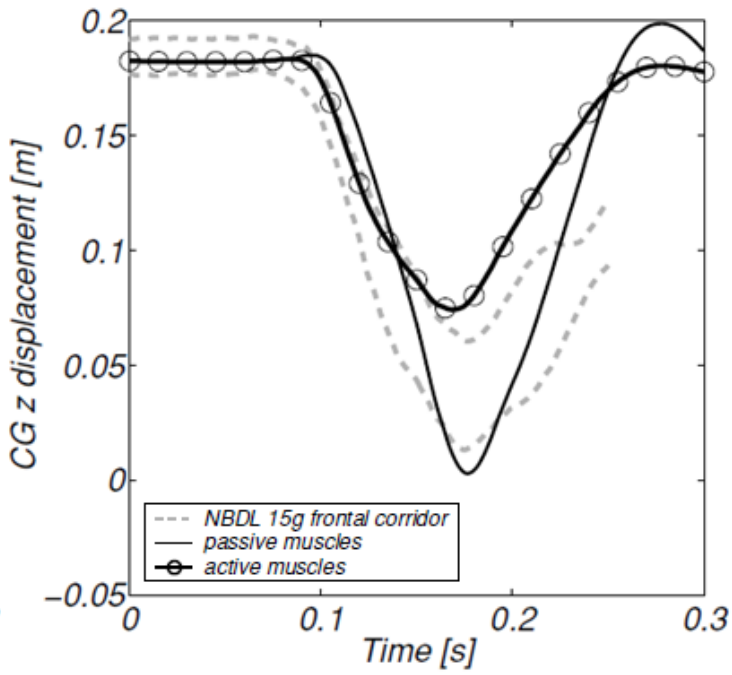

Figure 73. Displacement of Head cg with respect to torso in z direction (expressed in torso frame) compared with volunteers corridor Model of Van Der Horst (Adapted From [1])

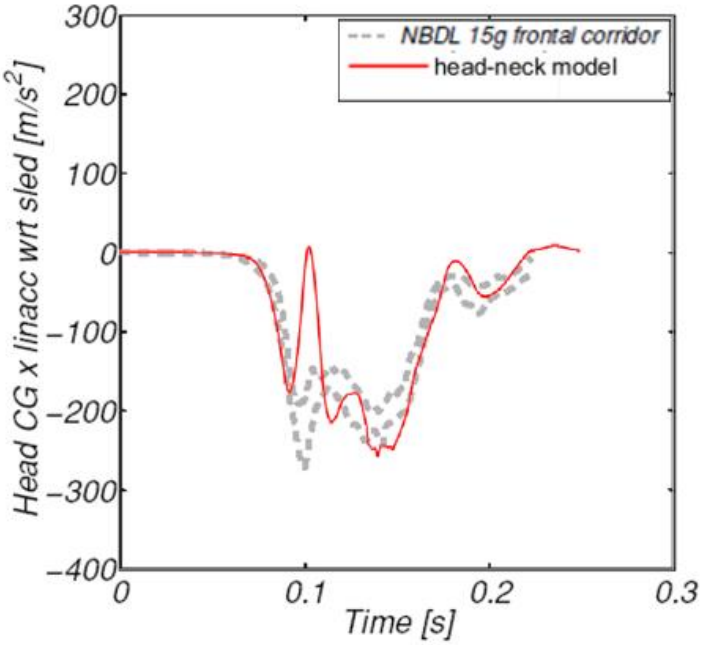

Figure 74. Head cg acceleration relative to sled in x direction compared with volunteers corridor

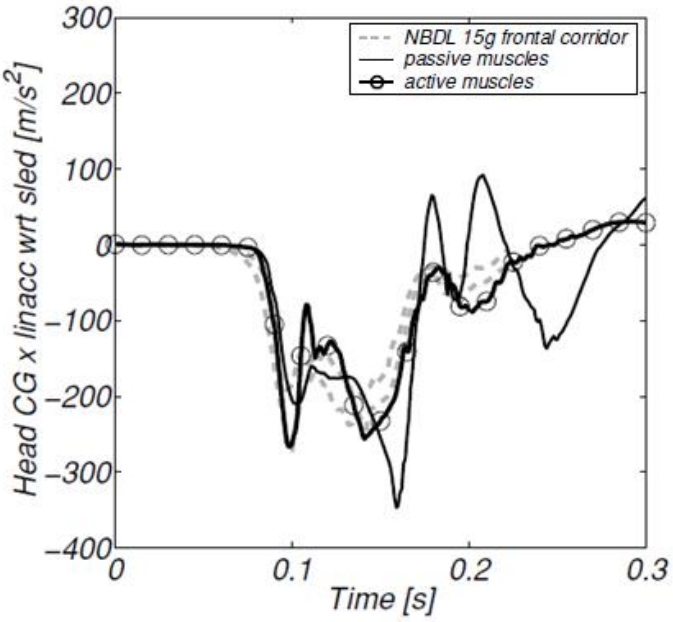

Figure 75. Head cg acceleration relative to sled in x direction compared with volunteers corridor Model of Van Der Horst (Adapted From [1])

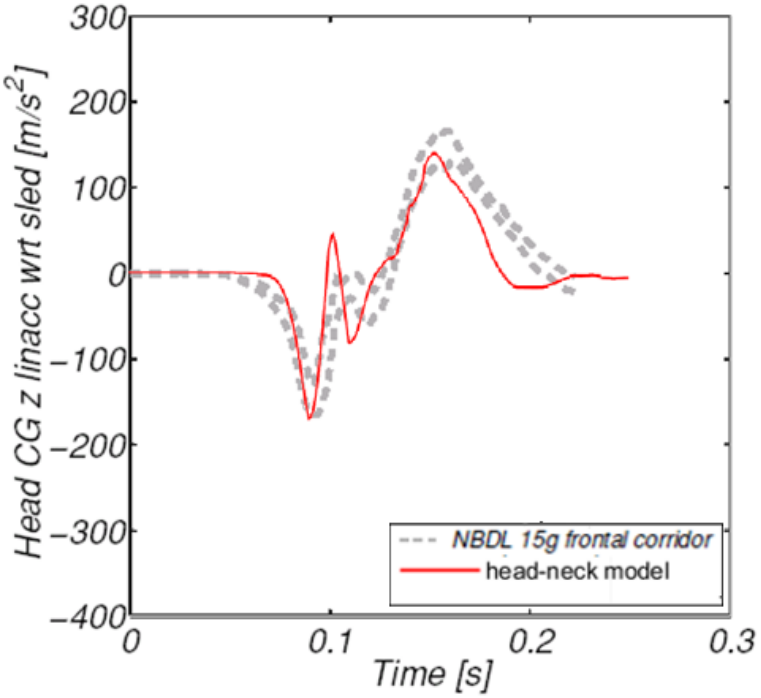

Figure 76. Head cg acceleration relative to sled in z direction compared with volunteers corridor

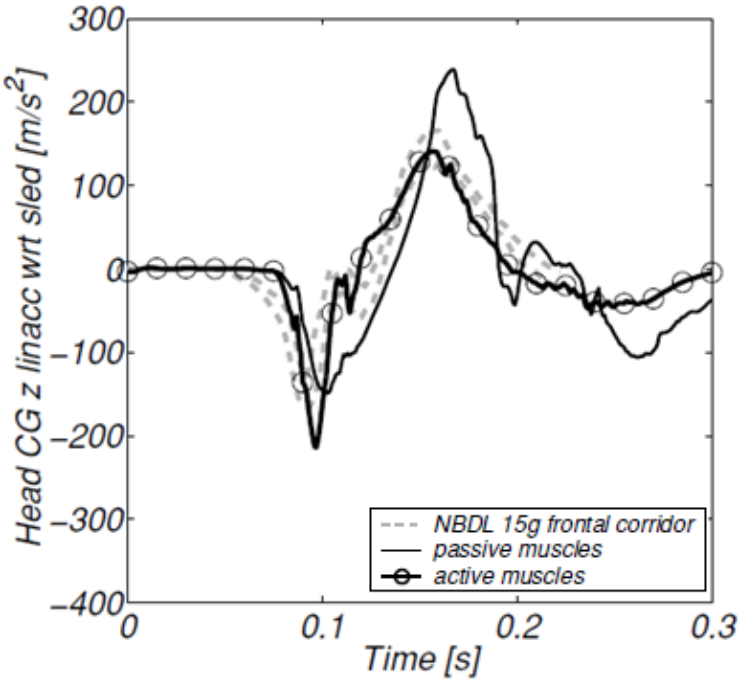

Figure 77. Head cg acceleration relative to sled in z direction compared with volunteers corridor Model of Van Der Horst (Adapted From [1])

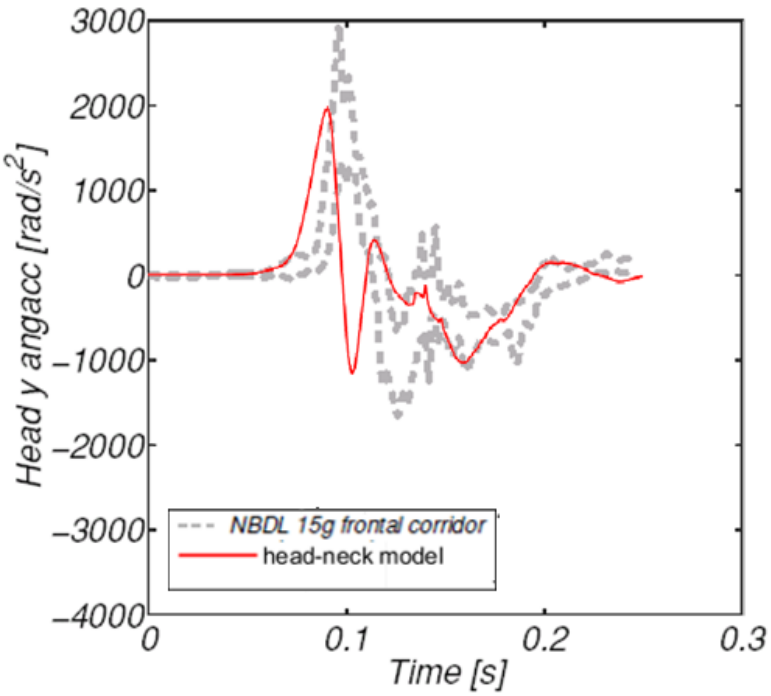

Figure 78. Head angular acceleration relative to inertial frame compared with volunteers corridor

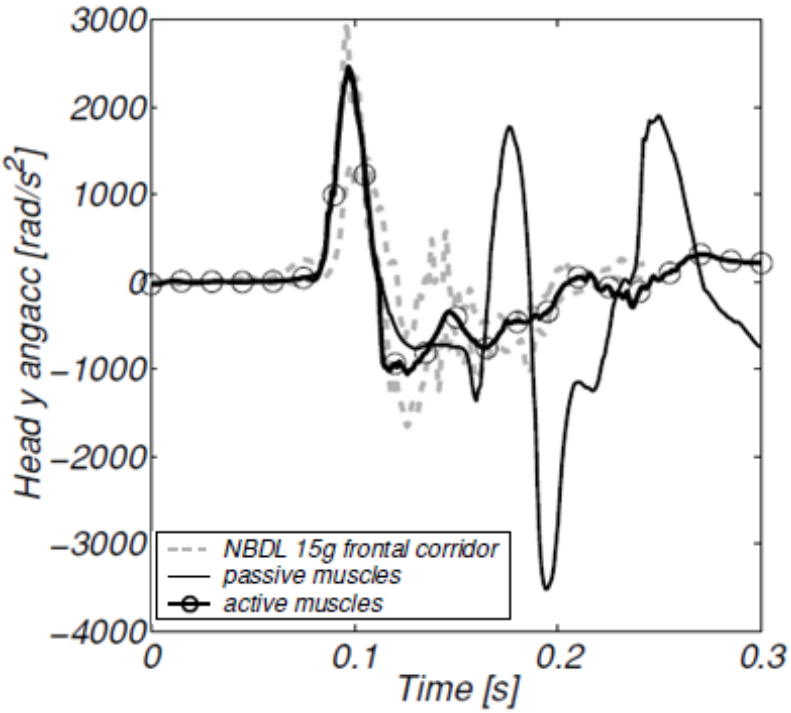

Figure 79. Head angular acceleration relative to inertial frame compared with volunteers corridor Model of Van Der Horst (Adapted From [1])

As seen on figures head and neck model are in good agreement with response corridors.

6. CONCLUSION AND DISCUSSION

This work aims a head and neck model to be used for both frontal and rear impacts. The model gives plausible responses comparing with cadaver rear impact tests as well as with volunteer rear impact tests and with volunteer frontal impact tests available in the literature.

There might be some source errors as given below which could alter the responses of the head and neck model:

When cadaver data is employed, average response is chosen instead of single ones since initial parts of cadaver response graphs i.e, 0 ms to 10-20ms, are hard to differentiate one from another. Small changes at the beginning of the simulations could give rise to big alteration of the motion response. Even if the data taken is correct, average cadaver responses do not represent individual ones. Fig. 80 is given as an example of this source error.

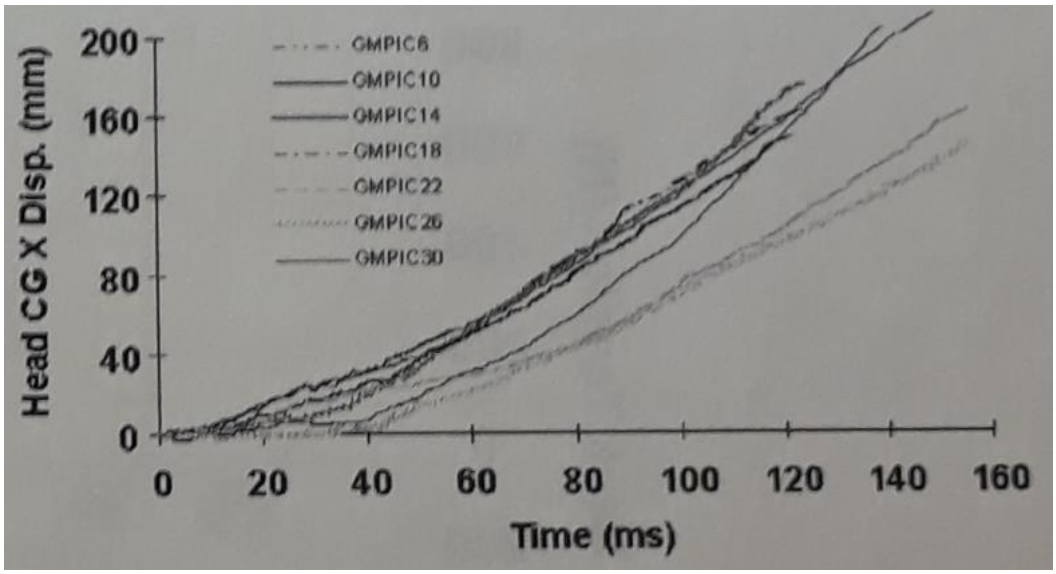

Figure 80. Individual cadaver responses of head center of gravity displacement in x direction low severe impact at T6 [5]

There is not enough information regarding initial orientation and initial displacements in the tests. Although initial orientation is taken same as in this work, it is possible that there was some minor difference betwen head orientation and torso orientation as just before the impact, shoulders of cadavers were hanged by wires for support and the head was kept in place by tiny pieces of tape [5]. Once pendulum hits on the back of the specimen, that tape strips properly leave on time is crucial for a healthy experiment and this might be difficult.

It should be noted that this is a dummy model. Even though cadavers are not live people, their spine was protected as possible as on the experiments. Therefore head neck response of cadavers behave as head-neck of a live person without active muscle. Since dummies are of basic designs there might be minor errors comparing with cadavers

It should also be considered that geometry of dummy vertebrae are simplier version of real vertebrae. Between real vertebrae there are not only rotational stiffness and damping in the motion of head-neck spine but also there are translational stiffness and damping, as well even though it has small amount of effect in the motion.

On frontal impact responses, Oc displacement with respect to torso in z direction deviates more than the others. Since there is no acceleration input in z direction on t1, this might have changed the response

REFERENCES

1. **van der Horst, M. J.** *Human head neck response in frontal, lateral and rear end impact loading: modelling and validation*. PhD Thesis, Eindhoven. University of Technology, Eindhoven, The Netherlands,2002

2. **de Jager, M. K. J.** *Mathematical head-neck models for acceleration impacts*. PhD Thesis, Eindhoven University of Technology, Eindhoven, The Netherlands, 1996

3. **Sato, F.; Nakajima, T.; Ono, K.; Svensson, M.Y.; Brolin, K.; Kaneoka, K.** *Dynamic Cervical Vertebral Motion of Female and Male Volunteers and Analysis of its Interaction with Head/Neck/Torso Behavior during Low-Speed Rear Impact.* Proceedings of the 2014 Ircobi Conference, Berlin, Germany, paper IRC-14-31, 227-249., 2014.

4. **Ono, K; Kaneoka K.** *Motion analysis of human cervical vertebrae during low speed rear impacts by the simulated sled*, *Proceedings of IRCOBI Conference*, 1997, Hanover, Germany.

5. **Viano, D. C., Hardy W. N.,** and **King, A. I.** *Response of the head, neck and torso to pendulum impacts on the back*. *Crash Prevention and Injury Control*, 2001, **2**(4), 289–306.

6. **Hoover, J., Meguid, S.A.** *Analytical viscoelastic modelling of whiplash using lumped-parameter approach*. *Int J Mech Mater Des* **11,** 125–137 (2015).

7. **van Lopik, D. W.** *A computational model of the human head and cervical spine for dynamic impact simulation.* PhD Thesis, Loughborough University Loughborough, UK, 2004.

8. **Jakobsson, L., Norin, H., Jernström, C., Svensson, S.-E., Johnsen, P., Isaksson-Hellman, I.,** and **Svensson, M. Y.** *Analysis of different head and neck responses in rear-end car collisions using a new humanlike mathematical model*. In Proceedings of International IRCOBI Conference, 1994, Lyon, France, pp. 109–125.

9. **van den Kroonenberg, A., Thunnissen, J.,** and **Wismans, J.** *A human model for low-severity rear- impacts*. In Proceedings of International IRCOBI Conference, Hannover, Germany, 1997, pp. 117–132.

10. **Yamazaki, K., Ono, K.,** and **Kaneoka, K.** *A simulation analysis of human cervical spine motion during low speed rear-end impacts*. SAE paper 2000-01-0154, 2000.

11. **Linder, A.** *A new mathematical neck model for a low-velocity rear-end impact dummy: Evaluation of components influencing head kinematics*. *Accid.* neck*Analysis and Prev.*, 2000, **32**(2), 261–269.

12. **Stemper, B. D., Yoganandan, N.,** and **Pintar, F. A.** *Validation of a head–neck computer model for whiplash simulation*. *Med. Biol. Engng Computing*, 2004, **42**(3), 333–338.

13. **Battaglia, Salvatore, Kajetan Kietlinski, Michiel Unger and Martin G.A. Tijssens.** *Occupant Protection in Rear-End Collisions Preceded by Autonomous Emergency Braking Deployment.* (2015).

14. **Himmetoglu S, Acar M, Taylor AJ, Bouazza-Marouf K.** *A multi-body head-and-neck model for simulation of rear impact in cars.* Proceedings of the Institution of Mechanical Engineers, Part D: Journal of Automobile Engineering. 2007;221(5):527-541.

15. **Huang, Tsai-Jeon ; Wu, Jun Tai.** *An ATD neck model based on multi-body dynamics subjected to rear impact.* In: Journal of Medical and Biological Engineering. 2009 ; Vol. 29, No. 3. pp. 152-157.

16. **Fice JB, Cronin DS, Panzer MB.** *Cervical spine model to predict capsular ligament response in rear impact*. Ann Biomed Eng. 2011;39(8):2152-2162.
doi:10.1007/s10439-011-0315-4

17. **Bertholon, N.,** *Finite element model of the human neck during omni-directional impacts.* PhD thesis, 1999. In French.

18. **Camacho, Daniel Luis Astilla.** *Dynamic Response of the Head and Cervical Spine to Near-Vertex Head Impact: An Experimental and Computational Study.* Order No. 9825625 Duke University, 1998. Ann Arbor: ProQuest. Web. 15 Aug. 2022.

19. **Dauvilliers,F., Bendjellal, F., Weiss, M. , Lvaste, F. Et al.** *Development of a Finite Model of the Neck*, SAE Technical Paper 942210, 1994

20. **Ejima, S. ; Ono, K. ; Kaneoka, K.et al.** *Development and validation of the human neck muscle model under impact loading.* International IRCOBI Conference on the Biomechanics of Impact, Proceedings. 2005. pp. 245-255

21. **Williams, J. L., & Belytschko, T. B.** *A three-dimensional model of the human cervical spine for impact simulation*. Journal of biomechanical engineering, 105(4), 321–331. (1983)

22. **Thunnissen, J.G.M. ; Wismans, J.S.H.M. ; Ewing, C.L. et al.** *Human volunteer head-neck response in frontal flexion : a new analysis*. 39th Stapp Car Crash conference proceedings : [San Diego, California, November 8-10, 1995]. Warrendale : Society of Automotive Engineers (SAE), 1995. pp. 439-460 (SAE-P).

23. **Himmetoglu, S.** *Integration of Muscle tone into a Multi Body Head and Neck Model for Crash Applications.* Proceedings of 26th International Scientific Conference. Transport Means (2022).

24. Haffner, M.P., Eppinger, R.H., Rangarajan, N., Shams, T., Artis, M., & Beach, D. (2001). *Foundations and elements of the NHTSA Thor ALPHA ATD design.*

25. Himmetoglu, S., Balci.T, Aydogan,M. *Validation of a Simple Multi-Body Head and Neck for Efficient Rear Impact Solutions.* Proceedings of 24th International Scientific Conference. Transport Means (2020).

26. Hulkey, F.H and Nusholtz, S.G, *Cervical spine biomechanics: A review of the literature.* Journal of orthopaedic research 4:232-243, Raven Press, New York(1986)

27. Kim, A., Anderson, K. F., Berliner, J., Bryzik, C., Hassan, J., Jensen, J., Kendall, M., Mertz, H. J., Morrow, T., Rao, A., & Wozniak, J. A. (2001). *A Comparison of the Hybrid III and BioRID II Dummies in Low-Severity, Rear-Impact Sled Tests*. Stapp car crash journal, 45, 257–284. https://doi.org/10.4271/2001-22-0012